LAPPEENRANTA-LAHTI UNIVERSITY OF TECHNOLOGY LUT
School of Energy Systems
Energy technology

Otso Lehtinen

FACTORS AFFECTING THE NEW CORRELATION DEVELOPED FOR THE SAVONIUS WIND TURBINE

Examiners: Professor Teemu Turunen-Saaresti
Associate professor Aki-Pekka Grönman

ABSTRACT

Lappeenranta-Lahti university of technology (LUT)
LUT School of Energy Systems
Energy Technology

Otso Lehtinen

Factors affecting the new correlation developed for the Savonius wind turbine

Master's thesis

2020

81 pages, 25 figures, 9 tables and 1 appendix

Examiners: Professor Teemu Turunen-Saaresti

Associate professor Aki-Pekka Grönman

Keywords: Wind energy, Savonius wind turbine, SWT, vertical axis wind turbine, VAWT, correlation

Wind energy is one of the fastest growing forms of energy production. Even though wind turbine is an old invention, large-scale electricity generation using wind turbines is relatively new thing. Bringing electricity production close to consumption brings new challenges where lesser-known wind turbines can have advantages.

The Savonius wind turbine is a vertical axis wind turbine. It was designed by Sigurd Johannes Savonius in the 1920s Finland. The Savonius wind turbine is perhaps the simplest wind turbine model available. It was designed by splitting a cylinder in half in height and moving the halves slightly apart. Although the Savonius wind turbine design is simple, there is still a large number of variables that influence its performance. These variables can be simple design parameters that are present in every turbine, or they can be add-ons designed to increase the performance.

Performance is not one of the advantages of the Savonius wind turbine. Some advantages are simple design, relatively low noise production, independence from wind direction and low physical space requirements. To achieve wider adoption, the benefits of the Savonius wind turbine must be sufficiently convincing to overcome the low efficiency. Several studies have suggested a new correlation that predicts the performance of the Savonius wind turbine using typical terms related to wind turbine performance. Previously formed correlation curves have been either linear or polynomial. A total of 52 different figures were analysed in order to find the design parameters that affect the shape of the correlation most. Most of the typical parameters did not significantly affect the shape of the correlation curve. Almost all of the studied turbines ended up in a linear correlation curve and those that ended up in a polynomial curve had some unique parts in their design that were not present in other studies.

TIIVISTELMÄ

Lappeenrannan-Lahden teknillinen yliopisto (LUT)
LUT School of Energy Systems
Energiatekniikka

Otso Lehtinen

Savonius-tuuliturbiinille kehitettyyn uuteen korrelaatioon vaikuttavat tekijät

Diplomityö

2020

81 sivua, 25 kuvaa, 9 taulukkoa ja 1 liite

Tarkastajat: Professori Teemu-Turunen Saaresti
Apulaisprofessori Aki-Pekka Grönman

Hakusanat: Tuulienergia, Savonius-tuuliturbiini, pystyakselinen tuuliturbiini, korrelaatio

Tuulienergia on yksi nopeimmin osuuttaan kasvattavista energiantuotantomuodoista. Vaikka tuuliturbiini on hyvin vanha keksintö, sen käyttäminen sähköntuotannossa on suhteellisen uusi asia. Sähköntuotannon tuominen lähelle kulutusta luo uusia haasteita, joissa vähemmän tunnetuilla tuuliturbiineilla voi olla etuja.

Savonius-tuuliturbiini on suhteellisen uusi keksintö tuuliturbiinien keskuudessa. Savonius-tuuliturbiinin kehitti Sigurd Johannes Savonius Suomessa 1920-luvulla. Se suunniteltiin halkaisemalla sylinteriputki pystysuunnassa, jonka jälkeen puolikkaita siirrettiin hieman erilleen toisistaan. Yksinkertaisesta rakenteesta huolimatta Savonius tuuliturbiinin suorituskykyyn vaikuttaa suuri määrä sen rakenteeseen liittyviä mitoitusarvoja ja lisäosia.

Suorituskyky on Savonius-tuuliturbiinin heikoimpia puolia. Sen etuja ovat yksinkertainen rakenne, suhteellisen matala käyntiääni, tuulen suunnasta riippumaton energiantuotanto ja vähäiset tilavaatimukset. Jotta turbiinin markkinaosuutta voitaisiin kasvattaa, tulee etujen olla suuremmat kuin heikon hyötysuhteen tuomat kustannukset. Useassa tutkimuksessa on ehdotettu uutta korrelaatiota, joka ennustaa Savonius-tuuliturbiinin suorituskykyä turbiinille tyypillisten parametrien avulla. Korrelaation avulla turbiinin käyttäytymistä tietyissä ympäristöissä voitaisiin ennustaa huomattavasti helpommin. Tässä työssä käsitellyissä tutkimuksissa on löydetty sekä lineaarisia että polynomisia korrelaatiokäyriä. Selvitystä varten käytiin läpi 52 erilaista turbiinikokonaisuuden mittausta, jotta korrelaation muotoon liittyviä muuttujia löydettäisiin. Valtaosa tutkituista parametreista ei vaikuttanut korrelaation muotoon merkittävästi. Lähes kaikki muodostetut korrelaatiokäyrät olivat lineaarisia. Toisen asteen käyriin päätyvät tutkimukset käyttivät osittain uniikkeja rakenteita, joita ei ollut käytössä muissa tutkimuksissa.

ACKNOWLEDGEMENTS

I thank the supervisor of this thesis for supervising this thesis. I also thank the supervisor for providing this topic. In addition, I thank the examiners of this thesis for examining this thesis.

Lappeenranta, 18th June 2020

Otso Lehtinen

TABLE OF CONTENTS

SYMBOLS AND ABBREVIATIONS

Latin alphabet

C_P	power coefficient	[-]
C_T	torque coefficient	[-]
V_∞	freestream velocity	[m/s]
A	cross-sectional area	[m^2]
E	energy	[Wh]
P	power	[W]
R	radius	[m]
Re	Reynolds number	[-]
t	time	[s]
T	torque	[Nm]

Greek alphabet

λ	tip–to–speed ratio	[-]
ρ	density	[kg/m^3]
ω	rotational speed	[rad/s]

Abbreviations

CF	capacity factor
CFD	computational fluid dynamics
HAWT	horizontal axis wind turbine
SWT	Savonius wind turbine
TSR	tip–to–speed ratio
VAWT	vertical axis wind turbine

1 INTRODUCTION

To bring energy production closer to consumption, small-scale energy production methods with relatively good efficiency and low noise production are needed. The use of wind energy for renewable energy production causes a low amount of harmful emissions and safety issues. Wind turbines produce mechanical power by converting the kinetic energy of wind into mechanical energy with turbine blades.

The amount of convertible energy depends on multiple factors such as wind velocity and direction. Wind turbines mostly used in large scale energy production are typical horizontal-axis wind turbines (HAWT) with three blades. Horizontal axis wind turbines are suitable for large scale energy production due to possibility for a high output power and relatively high efficiency. Even though the most famous wind turbines are typical horizontal axis wind turbines, many completely different models exist. Most of the global resources towards wind energy goes to these commercial large-scale wind turbines. In addition to commercial large-scale electricity generation, there are also applications for other types of turbines. Urban areas with variable wind directions and velocities create a difficult environment for horizontal-axis wind turbines that need to face the wind to rotate. Small-scale vertical wind turbines can be more suitable to difficult wind conditions. Some variants of small-scale vertical axis wind turbines (VAWT) are able to self-start even at low wind speeds. Self-starting capabilities are important in applications where no electricity is available to start the turbine or wind speed varies, such as in urban environment.

This thesis focuses on vertical axis wind turbine called the Savonius wind turbine. In addition to the basic data of the turbine, a more in-depth overview of its design parameters and their impact on performance is analysed. A new performance-related correlation using some key variables related to performance of the Savonius wind turbine has been proposed by multiple studies. The correlation curve is reviewed by using data from numerous previously conducted experimental and numerical studies to find the factors that dictate its shape and accuracy.

The Savonius wind turbine was originally referred to as the s-rotor by, which was developed in Finland in the early 20th century. There are many different applications for the s-rotor, the most common of which is a vertical axis wind turbine. This thesis focuses mostly on the wind turbine side of the s-rotor hence it will be mostly referred to as the Savonius wind turbine (SWT). The Savonius wind turbine is one of the simplest wind turbines available.

1.1 Background

The story of the s-rotor began in 1924. The designer of the rotor was interested in a ship that used the Flettner rotor. The Flettner rotor uses a rotating cylinder or a sphere with wind to cause a vacuum on one side of the cylinder which applies a force on the rotor. This phenomenon is called the Magnus effect. Thrust is created perpendicular to the wind direction and cylinder axis. The Flettner rotor needed an external power source to rotate the rotor in order to produce thrust for the ship. This led into an experiment to make a wind rotor that could eliminate the need for the external power source. Savonius took a cylinder from a Flettner-rotor and cut it in half. Cylinder halves were then moved so that they formed the letter s. Circular end plates were added on top and bottom of the halves and a shaft was added to the centre. (Savonius, 1931, p. 334)

After testing the s-rotor, it was assumed that the pressure caused by the Magnus effect was dependent on the rotational speed of the rotor. To increase the rotational speed, the half-cylinders of the rotor were moved towards the axis to create a gap between the cylinders. This allowed air to flow from the concave side of the advancing half-cylinder to the concave side of the returning half-cylinder. This would increase the pressure on the returning side to reduce the drag caused by the vacuum. Introducing the gap near the axis increased the rotational speed and the pressure caused by the Magnus effect. (Savonius, 1931)

In order to start reviewing the performance of the SWT, experimental studies conducted by Savonius himself are first reviewed. Savonius performed multiple experiments with numerous variants of the s-rotor and other wind turbines. Tests were also performed for

other use cases outside wind energy. A journal article about the new s-rotor and its applications was published in 1931. (Savonius, 1931).

1.2 Scope

Determining the performance of a wind turbine is difficult task. There are numerous design parameters that affect how the air flow hits the blades of a wind turbine. Even though the Savonius wind turbine is one of the simplest designs available, its performance is difficult to model or predict based on theoretical assumptions. A large number of different design parameters that affect the turbine behaviour and performance exists.

Most of the research about Savonius wind turbines include experimental, numerical and theoretical studies. These three methods will be explored in this thesis. Experimental studies are expensive and time consuming which is why they are sometimes supported by numerical studies. Even experimental wind tunnel tests are just simulations of real wind conditions. Thorough numerical studies are also time consuming. Theoretical studies need the data from experimental and numerical studies to back them up. Wind tunnel experiments are a reliable way to provide relatively accurate data of the performance of a wind turbine. While the data is more accurate to real life scenarios, there is a limited amount of data available from these experiments.

Since the performance of the SWT is affected by a large number of variables, many experimental and numerical studies have been conducted to measure the performance of different SWT variants. Performance affecting parameters include the blade number, inclusion of the end plates, the blade arc angle, the rotor twist, the stator vanes, the number of stages, the aspect ratio, the overlap ratio, the blade shape factor and the central shaft. Reynolds number also has a large effect on the performance of the SWT. Reynolds number is a quantity used to define the nature of the flow of the air or other fluid.

1.3 Objectives

To determine how different design parameters of a wind turbine affect its performance, data from multiple studies is needed. Data from experimental studies is preferred whenever available due to a higher confidence in the results. A new correlation for the performance of the SWT has been suggested by multiple studies in the last two decades. With a simple correlation, modelling the performance of a wind turbine could become easier without having to rely on expensive wind tunnel experiments. Since the performance of a wind turbine is affected by many variables, the shape of the performance correlation can also be affected in some way depending on the wind turbine design. While many studies have studied the performance correlation, there are some key differences in the results. To find out how the performance correlation behaves when changing multiple design parameters of the Savonius wind turbine, a large amount of data from primarily experimental studies is needed.

The goal of this thesis is to find out what variables define the shape of the correlation for the performance of a Savonius wind turbine. Confirming the existence of this correlation would make theoretical studies about the wind turbine more precise since turbine performance could in some level be modelled in various conditions without the need for physical experiments.

2 WIND ENERGY

Global energy demands are rising continuously and interest towards cost-effective clean carbon-free energy sources is increasing. Wind energy is one of the fastest growing energy production methods. According to an IEA report, production capacity of renewable energy is going to increase by 50 % from 2019 to 2024. Wind power accounts one quarter of the total growth. Onshore wind energy is predicted to determine the majority of the growth. Figure 1 shows the share of the wind energy against total renewable energy capacity between years 2000 and 2018. (IEA, 2019)

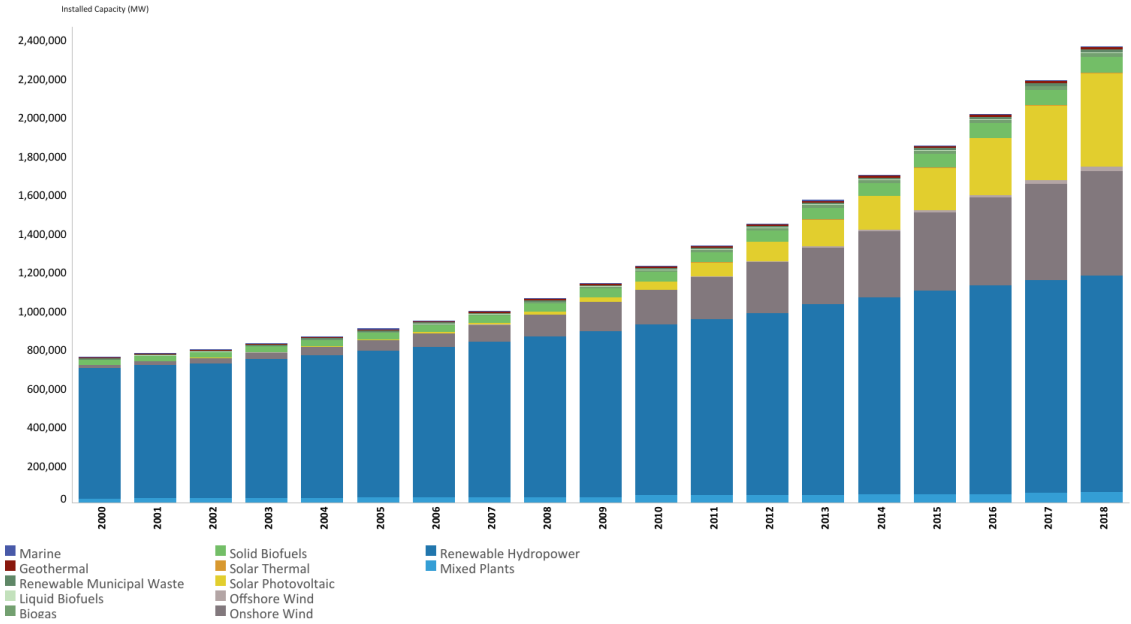

Figure 1. Global installed capacity of renewable energy from 2010 to 2018. Grey area shows the share of offshore and onshore wind energy. (IRENA, 2019)

Wind energy is energy obtained from air moving in the atmosphere. Wind velocity defines the amount of energy that can be obtained using wind turbines. Original source of the wind energy is solar energy. Radiation from sun divides unevenly on earth depending on multiple factors such as location, altitude and differences in energy absorption based on the properties of the absorbent material. Temperature and density differences create pressure differences. Due to pressure differences, air moves from higher pressure regions

to lower pressure regions. While radiation hitting Earth influences the amount of wind energy available, the atmosphere affects how much radiation Earth is able to absorb. (Kalmikov, 2017, p. 17)

Other reasons affecting the amount of wind energy are evaporation, precipitation, clouds, shade and dynamical forces caused by the rotation of the Earth. Different heat capacities of Earth materials lead to regional variation on amount of solar radiation absorption. Sea and land breezes are caused by differential heat capacities of water and soil. Scientific field that studies different wind phenomena is called meteorology. Due to physical differences, wind can be divided into different categories. Categories include geostrophic winds, thermal winds, gradient winds. Destructive wind systems such as typhoons or hurricanes are not useful for wind power generation. Wind turbines usually operate at much lower wind velocities. Wind can be divided into different types such as planetary scale, synoptic scale, mesoscale and microscale depending on the scale and spatial differences. Planetary scale includes global wind movements in the scale of tens of thousands of kilometers. Synoptic scale covers weather systems in lengths up to 1000 kilometers. Mesoscale includes regional wind movements from 10 to 100 kilometers. Microscale includes wind changes in range of 100 to 1000 meters. (Kalmikov, 2017, p. 18)

The amount of energy wind contains depends on wind flux. Flux is commonly used in fluid mechanics and it indicates a flow passing through an area. Since wind energy depends on continuous flow of air, efficiency can't reach 100 %. Theoretical maximum fraction of power that turbine is able to generate from wind is $C_p = 16/27 \approx 59$ % according to the Betz theory. (Kalmikov, 2017, p. 22)

2.1 Sustainability

Electricity production using wind energy does not produce greenhouse gas emissions after turbines are up and running. Wind energy is also free from other particle emissions caused by burning fossil fuels. Sustainability of wind energy depends on the efficiency of the wind turbines, the amount of building materials the turbine design requires, and the transportation required to transfer the parts of the wind turbine to the assembly site. Wind

energy is a long-lasting energy source since it depends on the solar radiation. Wind energy is widely available around the world. Ideal locations for large-scale wind turbine installations are typically windy and on high ground, which makes them less desirable for other purposes such as settlement. Distributing wind energy production depending where it is needed will reduce strains on the electricity grid caused by the centralized electricity production. On the other hand, large scale wind farms can be concentrated on either offshore or high-altitude areas which can lead to longer electricity transfer distances. (Trevor M. Letcher, 2017, pp. 8–10)

The cost of wind turbines has decreased significantly over time. Manufacturing process and other costs related to the electricity grid form a large part of the total investment costs related to a wind turbine. Due to the higher efficiency of taller wind turbines and efficiency gains due to the mass production of the wind turbines, the cost of wind energy is competitive with other energy sources. Energy used in the production process of a wind turbine can be generated back over a time of 7 months. A wind turbine can last 30 years of operation. Energy production with wind turbines is less dependent on other parties required in electricity generation such as fuel producers. (Trevor M. Letcher, 2017, pp. 8–10)

Wind energy production depends on wind conditions. The electricity grid requires a balance between production and usage. Due to fluctuations in wind conditions, large scale usage of wind energy can lead to imbalance between supply and demand. Storing can lead to massive losses depending on the method. Wind turbines produce noise pollution on some level depending on the size of the turbine. Since sound coming from a point source gets reduced exponentially as distance increases, the amount of noise is limited at modest distances. The sound pressure at 500 meters from the turbine can be around 35 decibels, which is very roughly equivalent to the sound of a whisper. Manufacturing process of a wind turbine requires a lot of building materials including some of the more rare materials that some parts like large magnets require. (Trevor M. Letcher, 2017, pp. 10–12)

Other possible concerns are limited harms caused to the wildlife population and flashing light levels created by large rotating structures. Harm to wildlife population can be very limited when compared to the harm caused by, for example, other animals or cars. Flashing lights caused by the rotor can cause epileptic symptoms on some people. Both of these problems are solvable by slowing down the rotational speed of the wind turbine rotor, which in turn can reduce the turbine efficiency. (Trevor M. Letcher, 2017, pp. 11–12)

2.2 Wind turbines

This section covers the basic information about wind turbines and their history as well as some terms related to the energy production. Wind turbines are machines used mainly for electricity generation. The kinetic energy from air is converted into mechanical energy of the wind turbine. Typically, a wind turbine contains at least a rotor, gearbox and generator. (Hau, 2013, p. 65)

2.2.1 Basics

The utilization of wind energy is extremely old technology. The origin from wind turbines starts from 200 B.C Persia. Later in the 7th century more modern wind turbines were developed in Iran. Original windmills harvested wind energy for lifting water and grinding corn until electricity producing windmills were designed originally in 19th century. Wind turbines were originally used to produce some electricity in 1930's USA. Later in 1950's John Brown & Co built first wind turbines connected to utility grid. (Tummala et al., 2016, p. 1351-1952)

Large scale electricity generation using wind turbines is a relatively recent thing. Production of wind turbines for electricity generation started in the 1970s with 500 kW turbines. Modern wind turbines can have output power of multiple megawatts with largest reaching up to 10 megawatts with even larger designs being planned. Although there are several different types of wind turbines, only horizontal-axis wind turbine has achieved a significant share of the global electricity generation capacity. The scale of wind turbines varies from small wind turbines under with output power of under kilowatt to large commercial

wind turbines with multiple megawatts of output power. Since the output power of a wind turbine depends on the sweep area of the rotor, the size of wind turbines is rising continuously. In addition, wind conditions are more favourable the higher the turbine is. (Trevor M. Letcher, 2017, p. 7)

Wind turbines can be divided into horizontal axis wind turbines (HAWT) and vertical axis wind turbines (VAWT). Wind turbines depend on lift and drag forces. Savonius wind turbine (SWT) is a typical example of a wind turbine that depends mainly on drag forces while horizontal axis- and Darrieus-wind turbines use lift forces. Wind turbines are also typically divided to small-scale and large-scale wind turbines.

Small-scale wind turbines typically have a power output of less than around 100 kilowatts. Small-scale wind turbines are usually not used in electricity production farms, but in other applications that require smaller size and cost. Wind conditions for small scale wind energy generation are difficult since wind velocity can be unstable and low at low altitude rural and urban areas with a lot of buildings and other obstacles. While the absolute cost of a small-scale wind turbine can be low, lower efficiency results in high relative costs. Noise production can be a problem since small-scale wind turbines are typically closer to the consumption. (James and Bahaj, 2017, p. 389)

There are both horizontal axed and vertical axed small-scale wind turbines. Vertical axis wind turbines include Darrieus and Savonius wind turbines. Due to design, HAWTs depend highly on wind direction, and need to be able to change direction continuously.

2.2.2 **Factors related to energy production**

Wind turbines gather energy from wind using drag and lift forces. Drag forces are main driving force, when applied force is in the same direction as the flow. Lift force is applied perpendicular to the flow. (Zemamou et al., 2017, p. 384)

Lift is caused by pressure difference between sides of the blade created by wind depending on the angle and shape of the blade. Pressure difference causes wind turbine blade to move towards the direction of the low-pressure side. (Trevor M. Letcher, 2017, p. 6)

Multiple key factors are used when defining wind turbine performance. Reynolds number (Re) is important dimensionless flow-related quantity of a fluid that shows the ratio of inertial forces to viscous forces (Whittlesey, 2017, p. 198). Reynolds number can be defined with following equation.

$$Re = \frac{\rho \cdot V_\infty \cdot D}{\mu} \quad (1)$$

where	ρ	is the density of the air,	[kg/m^3]
	V_∞	is the freestream velocity of the air,	[m/s]
	D	is the diameter of the rotor and	[m]
	μ	is the dynamic viscosity of the fluid.	[Pa·s]

Tip–to–speed ratio (TSR) is a ratio between rotor blade tip speed and freestream wind speed. TSR is defined with a following equation (Wenehenubun et al., 2015)

$$\lambda = \frac{R \cdot \omega}{V_\infty} \quad (2)$$

where	λ	is the tip–to–speed ratio of the rotor,	[-]
	R	is the radius of the rotor and	[m]
	ω	is the rotational speed of the rotor.	[rad/s]

Power coefficient (C_P) is a turbine power related factor which expresses how efficiently a wind turbine is able to convert energy from the wind. Power coefficient is unique to each turbine and is defined as the ratio of turbine power and wind power. Power coefficient can be calculated with a following equation. (Kalmikov, 2017, p. 22)

$$C_P = \frac{P_T}{\frac{1}{2} \cdot \rho \cdot A \cdot {V_\infty}^3} \quad (3)$$

where P_T is the power produced by the wind turbine and [W]

A is the cross-sectional area of the rotor. [m^2]

Torque coefficient expresses the ratio torque generated by the rotor and the maximum torque theoretically available on the wind. Torque coefficient is defined by a following equation.

$$C_T = \frac{T}{\frac{1}{2} \cdot \rho \cdot R \cdot {V_\infty}^2} \quad (4)$$

where T is the torque applied to the turbine shaft. [Nm]

Another key factor for the wind turbine performance measurement is the capacity factor (CF). The capacity factor refers to the ratio of energy produced to the maximum potential energy produced. Maximum potential energy is the amount of energy that can be generated during optimal wind conditions. The total amount of energy produced by a wind turbine over a period of time can be calculated by multiplying nominal power of wind turbine with time and capacity factor. Total produced energy over time is shown on equation 5. Capacity factor can be as high as 50 % in regions with favourable wind conditions. (Kalmikov, 2017, p. 23)

$$E_{produced} = P_{nominal} \cdot t \cdot CF \quad (5)$$

where $E_{produced}$ is the energy produced over the time t, [Wh]

$P_{nominal}$ is the rated power of the wind turbine and [W]

CF is the capacity factor. [-]

2.2.3 **Operational limits**

Wind turbines have key operating points on three different wind speeds. The speed at which turbine is able to produce any output power, maximum power output speed and point where turbine ends production due to too high wind speed.

Wind speed greatly affects power output of a wind turbine. Effect on wind turbines varies depending on the turbine model. Wind turbine power curve is a simple way to show how a typical wind turbine power output varies depending on the wind velocity. The following figure shows a typical wind turbine power curve. (Lydia et al., 2014, p. 453)

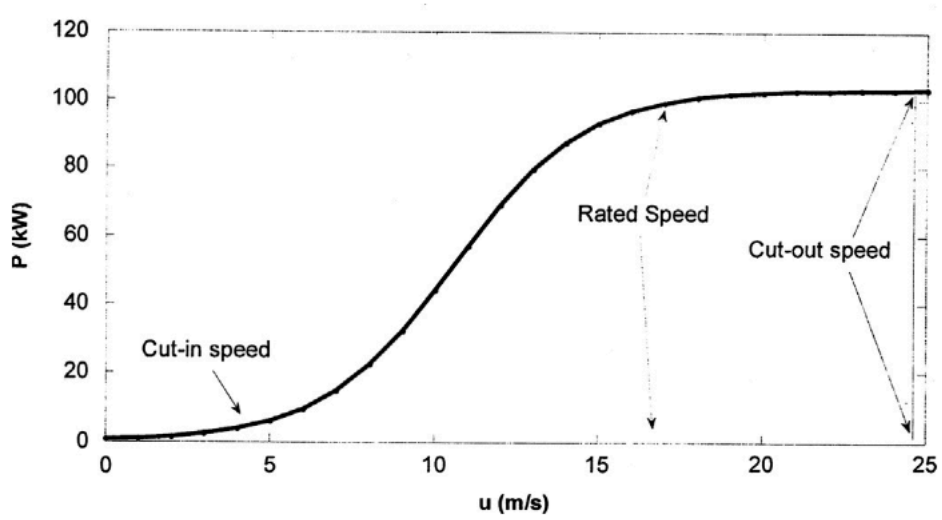

Figure 2. Typical wind turbine power curve. (Lydia et al., 2014, p. 453)

Methodology to measure wind turbine performance characteristics has been standardized by International Electrotechnical Commission (IEC). IEC 61400-12-1 is the international standard for power performance measurements of electricity producing wind turbines. The standard provides guidelines to measure different models of wind turbines. Measuring wind turbine performance includes simultaneous measurement of wind speed and wind turbine power output at those speeds. (Lydia et al., 2014, p. 453)

2.2.4 Offshore wind

Original offshore wind power plans originate from as far as 1930s Germany. Plans remained unfeasible for a long time due to technological and practical reasons. Plans remained inactive until 1973, when US Department of Energy and Department of Interior gave NASA means to start developing components essential for megawatt-scale wind turbines. Plans to reduce greenhouse gases especially after Kyoto Protocol has led to increased interest in offshore wind energy. Additionally, limited amount of usable land for wind energy has increased the interest towards offshore wind energy. (Poudineh et al., 2017, pp. 6–8)

Difficult marine conditions lead to considerably higher construction costs and higher equipment failure rates when compared to onshore wind turbines. Due to economic challenges, research and development on offshore wind energy has been limited. (Poudineh et al., 2017, p. 7)

Global demand of electricity is projected to grow into foreseeable future. A large part of global energy requirements come from coastal areas. Due to limited amount of land available, offshore wind power becomes attractive alternative to global energy requirements. Producing electricity locally also reduces stresses on the electricity grid. (Poudineh et al., 2017, pp. 10–11)

Offshore wind energy remains economically challenging solution to rising electricity consumption despite receiving increasing amount of interest and development resources. As technology matures, building costs tend to go down. Since offshore wind energy has received relatively small research and development resources, there is room for the costs to decrease over time. (Poudineh et al., 2017, p. 13)

2.2.5 Horizontal axis wind turbines

Horizontal axis wind turbines (HAWT) use blades that rotate around a horizontal axis. HAWT design includes a number of blades facing wind at certain blade angle to take advantage of lift forces. Figure 3 shows typical horizontal axis wind turbine components.

The figure also shows the yaw angle system where a wind vane and an anemometer are used to determine the direction of the wind. HAWTs are the most widely used wind turbines for large scale power generation and gather a large part of the wind energy development resources. This is due to the higher power coefficients and power output of HAWTs. The higher power coefficient is achieved with the ability to continuously produce power with all of the blades at the same time. (Johari et al., 2018, p. 75)

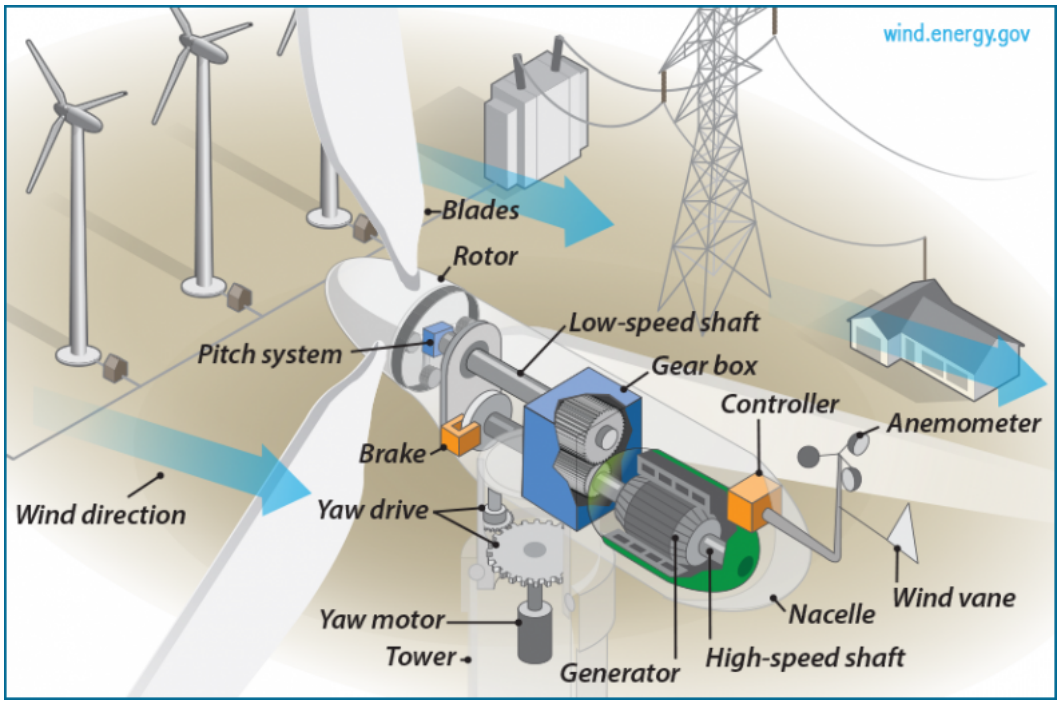

Figure 3.Typical components of a horizontal axis wind turbine. (U.S. Department of Energy, n.d.)

Since the blades need to face the wind, the turbine must be able to change the yaw angle according to the wind direction. For small wind turbines, a simple vane at the end of the turbine gearbox is enough to change the direction. Larger turbines need a way to figure out the optimal yaw angle for optimal performance. Motorized machinery is needed to change the yaw angle. Due to the challenges related to the yaw angle, the optimal environment for the HAWT design has consistent wind velocity and direction with low turbulence. The size of HAWTs as a function of time is illustrated in figure 4. (Johari et al., 2018, p. 75)

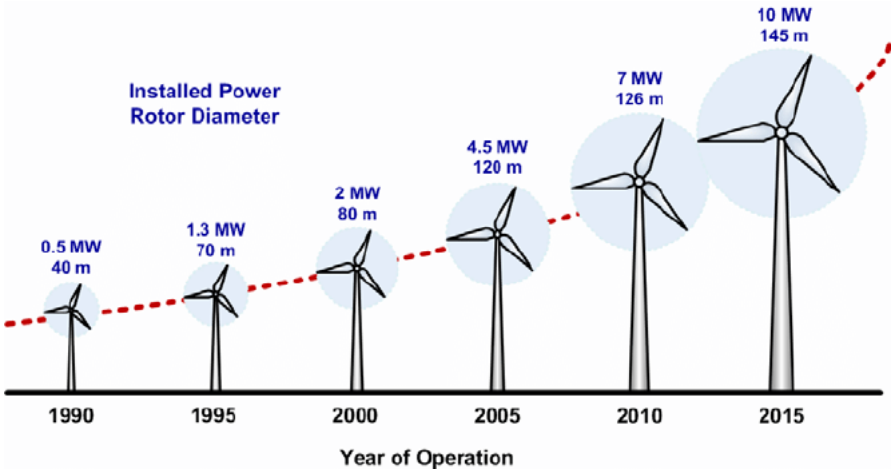

Figure 4. Size of horizontal axis wind turbines as a function of time between 1990 and 2015. (Molina and Mercado, 2011, p. 376)

Material strengths are a problem for higher power HAWTs. Longer blades in high power HAWTs require high material strength. Rotating blade undergoes a lot of bending stresses from multiple angles. Increasing strength of the blade by increasing the amount of building materials also leads to higher bending stresses due to gravity. Higher amount of building materials also leads to increased manufacturing costs and emissions from turbine production. Higher weight of the rotor increases the amount of bending stresses on the wind turbine tower. The tower also needs to withstand the material stresses from all directions due to changing yaw angle of rotor. (Tjiu et al., 2015, pp. 560–561)

Weight of wind turbine components can be affected with building materials. Typical high power HAWT uses glass fibre to increase material strength while keeping it relatively lightweight. Carbon fibre is used in some parts of the turbine, where increased strength to weight ratio is needed. Wider usage of carbon fibre would lead to exponentially higher building costs. (Tjiu et al., 2015, p. 561)

Other challenge for high power HAWTs is the construction process. Components of a wind turbine need to be transferred to the building site which requires a good road access. Transportation costs increase rapidly the longer the turbine blades are. (Tjiu et al., 2015, p. 562)

2.2.6 **Vertical axis wind turbines**

Vertical axis wind turbine (VAWT) axis is in vertical orientation. VAWT is the oldest wind turbine design. Original VAWTs only used drag forces to rotate (Tummala et al., 2016, p. 1364). Nowadays there are models using either drag forces, lift forces or both (Whittlesey, 2017, p. 189). VAWT design allows the storing of the electrical equipment on the ground level and no need for a system to change the turbine yaw angle (Hau, 2013, p. 66).

Two most common vertical axed designs are the Savonius wind turbine (SWT) and the Darrieus wind turbine (DWT). Although both of the turbines are built around a vertical axis, they are still fundamentally two completely different designs (Abraham et al., 2012, p. 4). A combined Darrieus-Savonius wind turbine design is also possible, whereby SWT is used to start the DWT. Figure 5 shows three different VAWT variations: the SWT, the DWT and the H-rotor variation of the DWT.

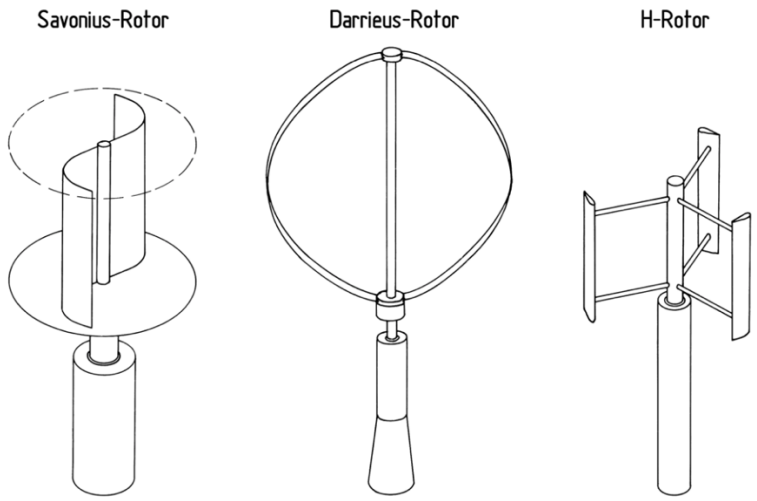

Figure 5. The Savonius VAWT, the Darrieus VAWT and the H-rotor, a variation of the Darrieus VAWT. (Hau, 2013, p. 66)

The SWT is a simple wind turbine design that uses drag forces to rotate. SWT was designed by a Finnish engineer Sigurd Johannes Savonius (Tummala et al., 2016, p. 1364).

Savonius wind turbine is a simple and robust design suffering from a low efficiency due to its reliance on drag forces. Since SWT relies on drag forces, only the blade advancing with the air flow produces positive torque to the generator. Negative torque is caused by the returning blade. Due to the shape of the blades, the positive torque caused by the advancing blade is greater than the negative torque caused by the returning blade. To optimize the SWT performance, the difference between positive and negative torque should be maximized. In order to achieve a higher efficiency with VAWT design, the blade should be able to produce positive torque throughout the cycle. (Whittlesey, 2017, pp. 189–190)

The Darrieus wind turbine is a VAWT that is able to utilize lift forces. Darrieus VAWT was designed in France in 1931 by engineer Georges Jean Marie Darrieus. The efficiency of the DWT is relatively high for a VAWT due to the usage of lift forces that allow the blades to produce positive torque throughout the cycle (Tummala et al., 2016, p. 1360). Due to the shape of its blades, the design of the Darrieus VAWT is much more complicated than SWT. Complicated design makes manufacturing of DWT more expensive. DWT is also unable to control its output power by changing the blade pitch due to the complex shape of the blades. DWT has a more simple variation called the H-rotor which uses straight blades instead of the curved ones on the typical design. (Hau, 2013, pp. 66–68)

The cup anemometer is another VAWT which is used to measure wind velocity. The cup anemometer uses multiple hemispherical cups placed around a vertical axis to rotate regardless of the wind direction. (Hau, 2013, p. 66)

Due to the vertical axis design, turbine yaw angle does not need adjusting according to wind direction. This gives VAWT an advantage in variable wind conditions. Vertical axis wind turbines produce less noise compared to horizontal axis wind turbines. Design also allows to store electrical and mechanical component at ground level. (Hau, 2013, p. 66)

Due to the higher drag caused by the design of VAWTs, tip–to–speed ratio and efficiency is lower than that of horizontal axis wind turbines (Tummala et al., 2016, p. 1354). Development of the VAWT design has been relatively slow. Complex design of DWT and disadvantages related to efficiency especially on Savonius wind turbine made HAWT a more compelling choice for development resources (Hau, 2013, p. 69).

Some of the vertical axis wind turbines, mainly DWTs, are unable to self-start. DWT is unable to produce positive torque at certain range of tip–to–speed ratios. To overcome the negative torque at the beginning, electrical motor is used to drive the turbine until it is able to sustain rotation. HAWTs and drag-based VAWTs are able to self-start if certain wind speed is achieved. Since drag-based VAWT is able to self-start with low wind speeds, the self-starting capability of the DWT can also be achieved by combining it with a drag-based wind turbine. In this case, the drag based turbine can lower the aerodynamic efficiency of the DWT. (Whittlesey, 2017, pp. 193–194)

3 SAVONIUS WIND TURBINE

Sigurd Johannes Savonius published his research about the Savonius wind turbine (SWT), or as it was originally called, the s-rotor, in 1931. The goal of the s-rotor was not to achieve the highest efficiency like many other projects did at the time. The goal was to introduce a turbine design that could work in constantly changing wind direction without the need for correcting the yaw angle. (Savonius, 1931, p. 333)

The Savonius wind turbine is one of the simplest VAWT designs available. The SWT is vertical axis wind turbine that mostly uses drag forces for power generation. Due to the low aerodynamic performance, the SWT is not very appealing choice for large scale energy production. While the turbine may be unsuitable for large-scale production, there are numerous applications that the SWT has advantages. Simple and inexpensive design paired with a relatively high starting torque combined with self-starting capabilities at low wind speeds without dependence on wind direction can make the SWT an attractive choice for distributed power generation applications.

3.1 Working principle

The design of the SWT is a simple vertical axis wind turbine. The typical SWT uses only drag forces for energy production since blades of the SWT are perpendicular to the wind flow and in the same direction as the turbine axis. Due to its dependence on drag forces, the performance of SWT starts to deteriorate after certain rotational speed. This is due to blade tangential velocity exceeding the velocity of the air flow leading to loss of momentum into the air. (Akwa et al., 2012, p. 3056)

In addition, by relying on drag forces, the efficiency of the SWT is fairly low. The low efficiency is due to the negative torque caused by the returning blade of the rotor. The drag forces apply to both blades at the same time. Due to the curved blade design, the torque caused by the advancing blade is higher than that of the returning blade which leads to rotation caused by the positive total torque. Since blades of the SWT produce torque for only half of the revolution while the other half is causing negative torque, SWT

performance coefficient is lower than that of lift-based wind turbines. In order to improve the performance of the SWT, torque difference between advancing and returning blade should be maximized. (Abraham et al., 2012, p. 8)

3.2 Design and dimensions

The design of the Savonius wind turbine includes two cylindrical blades between round end plates. These two blades can have some separation distance between each other. Another important dimension is overlap-ratio, which indicates, how much two blades overlap each other. (Abraham et al., 2012, p. 4)

Numerous parameters can be optimized or added to modify the performance of the SWT. Parts commonly used in Savonius wind turbine are blades, end plates, stator, blade curtain, obstacle shielding. Other parameters related to the SWT are presented in figure 6.

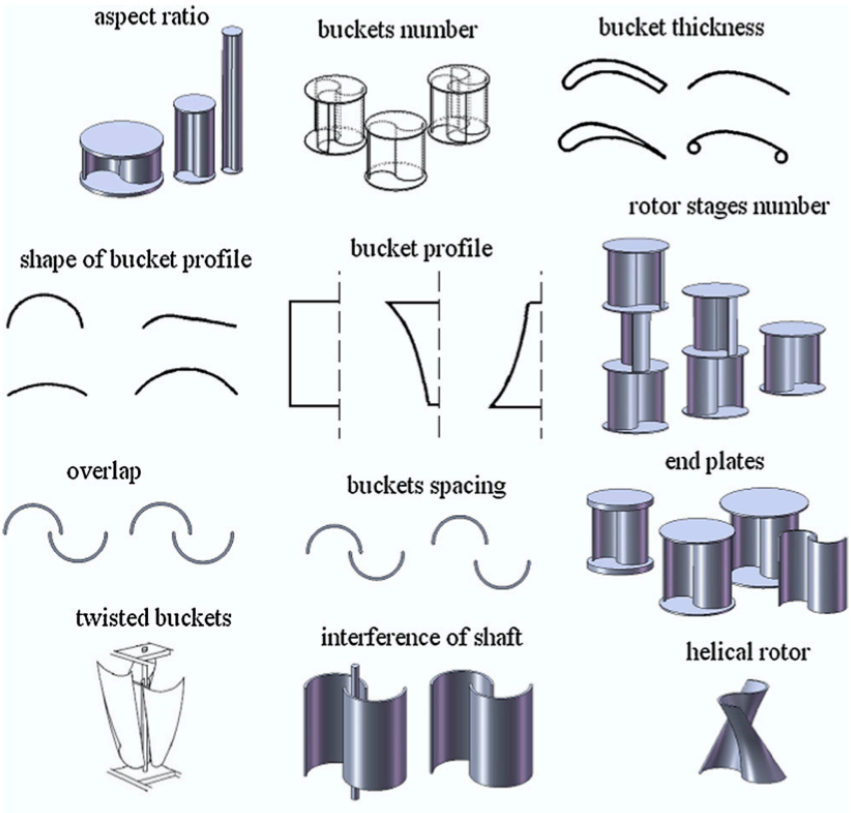

Figure 6. Savonius wind turbine design parameters. (Akwa et al., 2012, p. 3059)

Figure 7 visualizes Savonius wind turbine rotation and some of its dimensions. Dimensions are marked with letters. In figure, a is the blade radius, b is the overlap distance, c is the spacing between the blades, d is the inner diameter of the rotor, e is the endplate diameter, f indicates the wind direction, g indicates the direction of rotation and h is the straight part of the blade.

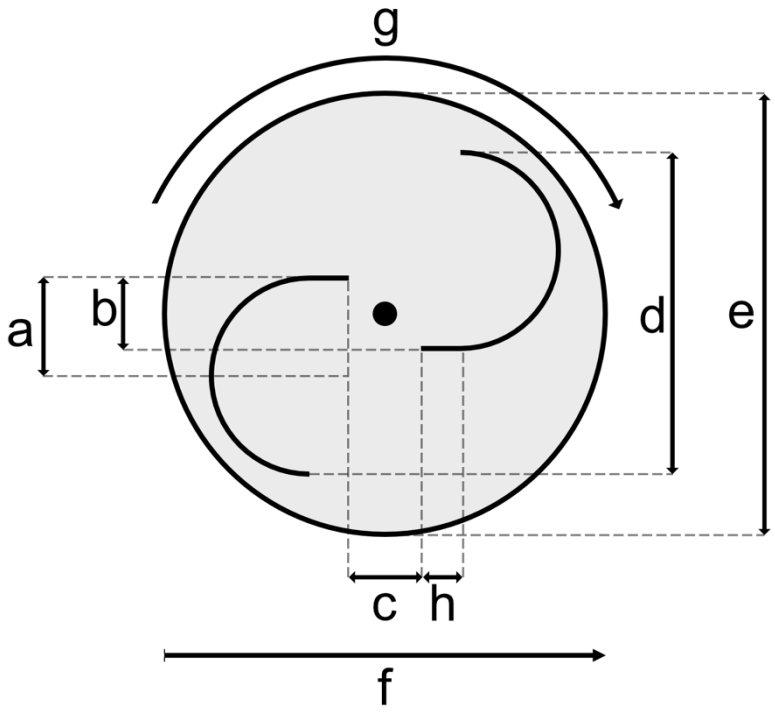

Figure 7. Savonius wind turbine rotation direction and different parameters of the rotor. In the figure, a is the blade radius, b is the overlap distance, c is the spacing between blades, d is the inner diameter of the rotor, e is the endplate diameter, f indicates the wind direction, g indicates the direction of rotation and h is the straight part of the blade.

Some designs covered in this thesis are called Bach-type VAWTs. A Bach-type is a variation of the Savonius wind turbine with slightly different dimensions. The Bach-type rotor includes two semi-circular blades with a straight part added to the inner edge of the arc as indicated with a letter h in the figure 7. The straight blade area can also connect those two blades together which means there is no overlap distance or spacing between blades. (Zhou and Rempfer, 2013, p. 374)

3.3 Applications

This section covers possible use cases for Savonius wind turbine that no other turbine type is as suitable to be used. Sigurd Johannes Savonius wrote about potential use cases for the s-rotor. Applications covered in this section are mainly related to the wind turbine, but some applications are listed from other areas of the s-rotor. Horizontal axis wind turbines require a relatively steady wind flow and depend on the wind direction. This opens potential applications for Savonius wind turbine in locations where varying wind conditions are expected.

There are many potential use cases for the s-rotor. Some applications described by Savonius are listed in table 1. Not all of these applications are related to the Savonius wind turbine, which is discussed in more detail in this section. (Savonius, 1931, p. 336)

Table 1. Use cases for the s-rotor described by Sigurd Johannes Savonius (Savonius, 1931, p. 336).

Pumping and electricity generation
Pressure and exhaust fans
Moving signs outside
Automobile mascot
Propelling toy rotor ships
Air and water stream measuring
Driving gyros in airplanes
Generators and compressors
Water motors used with rivers and tidal waves
Wave motor

Potential use cases for the SWT are also places where HAWT cannot fit due to physical space constraints. Some potential applications are cellular towers or near highways and railways. Since Savonius wind turbine is able to start with relatively low wind speeds, it can be useful for small tasks such as starting other turbines that are incapable in self-starting (Morshed et al., 2013, p. 1).

Urban and rural areas are well suited for the SWT. A typical application for the SWT is attaching it to buildings and producing electricity locally. Buildings contain a lot of obstructions to the wind and are usually on low altitude which results in low wind speed. The SWT is able to start rotating on its own even on low wind speeds. These environments with limited space available can be impossible for large rotating blades of HAWTs making the compact size of the SWT beneficial. (Abraham et al., 2012, p. 5)

If Savonius wind turbine is placed close to a highway, vehicles moving at high speeds create potential drag forces that can be used for power generation. The SWT is suitable for this due to being able to generate power with low and constantly changing wind speeds. A low-cost SWT was used to test how vehicles affect wind speeds near highway in experimental study by Santhakumar et al. SWT performance was evaluated near two-lane highway at 1 m altitude. Depending on the road, nearby vehicles crossing by nearby SWT increased rotational speed by up to 57 %. Vehicles crossing near the SWT increased wind speeds by up to 40 % compared to original wind speeds. On the other hand, vehicles passing through at the opposite lane results in slightly reduced wind speeds. Using SWT near highway has some potential for power production, but it is also dependent of the location and opposite lane of the highway. (Santhakumar et al., 2018, pp. 6–11)

High-speed railway needs electronic devices along railway tunnels to ensure operational safety. Pan et al. studied possibility of harvesting wind energy in railway tunnels to power the required equipment. Experiments used Savonius s-rotor and H-rotor to harvest wind energy caused by passing train. Results of the experiment included maximum power output of 107.76 mW with maximum efficiency being 23.2 %. Windspeed was 11 m/s at the time. (Pan et al., 2019, p. 1)

Due to its ability to work in variable wind conditions and generate power with low torque, SWT could be used in street lighting system by integrating multiple high aspect ratio turbines into streetlamp. In this case, the support poles may affect the performance of the SWT negatively by causing flow separations. (Montelpare et al., 2018, pp. 146, 157)

Another potential application for the SWT is powering cellular towers around the world. According to the work by Abraham et al., modern cellular towers require around 1–3 kW of power. Since the Savonius wind turbine requires little physical space to work with, it can be installed to cellular towers to protect the network access in power outages. This would be useful especially in regions where grid power outages are common and in rural regions. In rural regions cellular towers can be powered locally with no connection to national electricity grid. (Abraham et al., 2012, pp. 6–7)

3.4 Performance

In this section, the performance and typical advantages and disadvantages of the Savonius wind turbine are analysed. Both the vertical axis design and the reliance on drag forces create clear disadvantages that need to be taken into account when designing application for a wind turbine. The design also comes with some clear advantages to other wind turbines. These will be examined later in this section. The performance of the SWT is affected by multiple design parameters. More detailed reviews of performance affecting design parameters that require a closer look will be examined in the next chapter.

After designing the s-rotor, Sigurd Johannes Savonius examined the performance of the rotor with numerous experimental investigations. To find the optimal design parameters for the s-rotor, a more spacious wind tunnel was needed. A total of around 50 different turbine models 30 of which were variants of the s-rotor. were tested in the new wind tunnel. The results for horizontal turbines were in line with other experimental studies. The best horizontal turbine achieved a power coefficient of 0.325. The best power coefficient by a vertical axis turbine was achieved with three-bladed variant of the s-rotor. The variant achieved a power coefficient of 0.14. After removing circular end plates, the power coefficient dropped down to 0.07. Adding more vanes than 3 further reduced the power output. The highest recorded power coefficient of any s-rotor variant was 0.31. While the best performance was achieved with a tip–to–speed ratio of 0.85, it varied between 0.65 and 1.74 in experiments. Though TSR of 0.85 achieved the highest performance, only 2–3 % reduction in power output was measured when TSR varied between

0.65 and 1.1. At the time of the experiment, theoretical maximum power coefficient for a vertical axis wind turbine was 0.2 of which only half could be produced in optimal real-life conditions. (Savonius, 1931, pp. 334–335)

After the experiments in the wind tunnel, the s-rotor performance was measured in natural wind conditions. As Savonius had predicted, the rotor power output was higher in these conditions as opposed to horizontal-axis wind turbines. Multiple tests showed a higher power coefficient of 0.37. Additionally, the losses caused by changing wind direction are not applied to the s-rotor. The optimal tip–to–speed ratio rose to 0.92–1.0 in natural wind conditions. (Savonius, 1931, p. 336)

The form of the s-rotor affects, how it rotates. A large diameter combined with short height produces more torque with slower rotational speed. On the other hand, short diameter combined with large height leads to less torque and higher rotational speed. (Savonius, 1931, p. 336)

Performance of SWT is relatively low compared to most other wind turbine designs due to its reliance on drag forces which in turn result in low tip–to–speed ratio. The low power coefficient of the SWT compared to other wind turbine types is illustrated in figure 8.

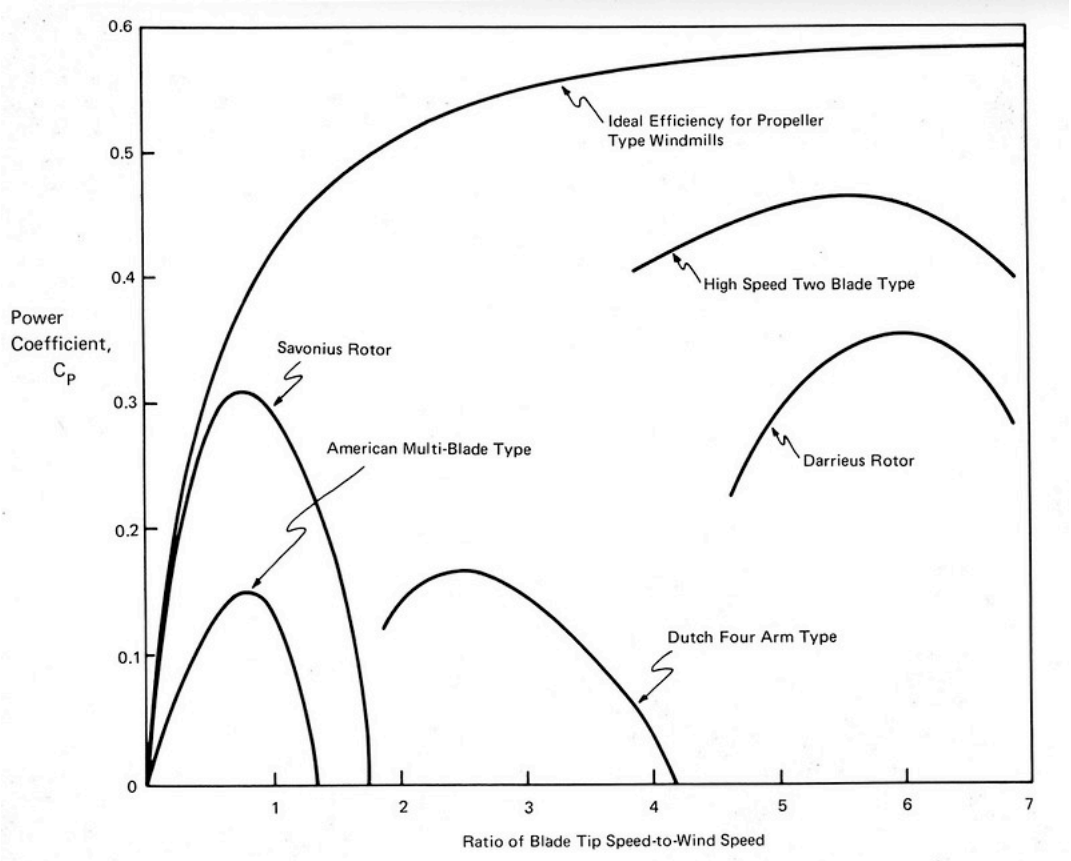

Figure 8. Power coefficients for different wind turbine types as a function of tip–to–speed ratio. (U.S. Department of Energy, 1977)

3.4.1 **Advantages**

The Savonius wind turbine has numerous clear advantages. The SWT is able to start rotating on its own even on low wind velocities. Due to relatively large starting torque, power generation is also possible with low wind velocity. The simple design of the SWT makes it easy and especially cost-effective to manufacture (Morshed et al., 2013, p. 1). The design of the SWT is also robust and produces less wear on the moving parts of the wind turbine which also leads to low maintenance costs. The basic configuration of the SWT can be modified in numerous ways to improve its performance, as shown in the figure 6.

Due to the vertical axed design of the SWT, no system is needed to control the yaw angle of the turbine. The SWT works in all wind directions (Abraham et al., 2012, p. 5). Since the SWT design relies less on the physical space and can operate in variable wind conditions, the turbine is better suited in urban environments for example. Those environments can have a lot of obstruction to wind, limited space and less tolerance for turbine noise (Abraham et al., 2012, p. 5). The SWT can be integrated into other structures such as high vertical structures fairly easily to provide alternative ways for power generation (Montelpare et al., 2018, p. 1).

Low aerodynamic noise is a critical factor when installing wind turbines close to residential areas. While noise emissions of small VAWTs are relatively low, continuous aerodynamic noise still exists. To be successful in residential and urban areas, low noise levels should be one deciding factor when designing SWTs. (Kim and Cheong, 2015, p. 199)

Due to the design, the physical space requirement of a VAWT is much lower than that of a HAWT. This gives VAWT an advantage on areas with limited physical space. Low space requirement makes it also possible to place multiple turbines much closer to each other. (Abraham et al., 2012, p. 5)

3.4.2 **Disadvantages**

Due to the design of a drag based VAWT, the aerodynamic efficiency is much lower when compared to lift-based turbines. The SWT is designed to be used near ground. Since potential energy in the wind is typically a lot higher in high altitudes due to higher wind speeds, the amount of power that the Savonius VAWT can generate relative to the power of the wind is limited. Partial solution would be to use existing tall constructs such as previously mentioned cellular towers. In this case, the availability of suitable high-altitude installation locations is limited. Installing wind turbine to another structure increases static and dynamic tensions to the structure. (Riegler, 2003, p. 1)

Higher power designs could be a key to make high-altitude instalments economically sustainable. Designing larger Savonius wind turbines would lead to high material usage

per area of wind covered compared to horizontal axis wind turbines. Increasing material usage would increase the weight and building costs for already relatively inefficient wind turbines. (Riegler, 2003, p. 1)

Another downside of the SWT is that the torque is not even throughout a revolution. Uneven torque is a problem especially for the SWT since it relies only on drag forces and has the basic design has only two blades. This disadvantage is something, that Savonius examined in the early experiments on the new rotor design. Uneven torque leads to higher starting torque on some rotor angles. Higher starting torque makes it difficult for the turbine to self-start under a load. Figure 9 shows the torque curve for the s-rotor and two other wind turbines. While torque curves of two other wind turbines shown in the graph are circles, the curve of the s-rotor is uneven and has distantly elliptical shape.

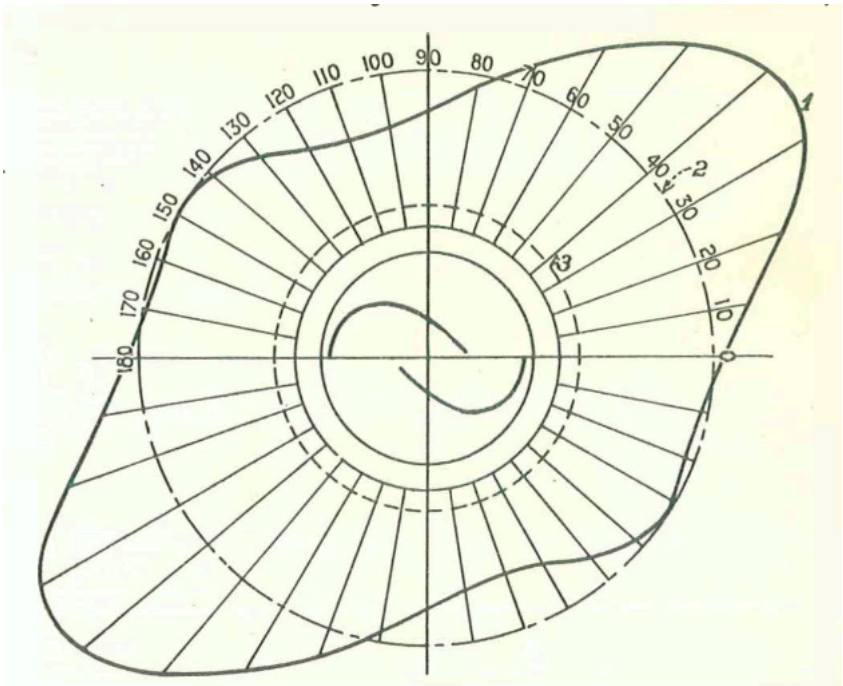

Figure 9. Torque of the s-rotor from every angle from the original study by Sigurd Johannes Savonius. The figure includes torque curves for the s-rotor (1), 12-vaned steel windmill (2) and 4-vaned La Cour mill (3). (Savonius, 1931, p. 335)

4 SAVONIUS WIND TURBINE PERFORMANCE

This chapter explains what different factors are affecting the performance of the Savonius wind turbine. A large number of experimental, numerical and theoretical studies have been done to monitor the performance of the SWT in different operating conditions.

Factors affecting the performance of the SWT are number of blades, inclusion of end plates, blade angle, twist, stator, number of stages, aspect ratio, overlap ratio, spacing and venting. Optimizing these factors will make SWT more appealing choice for energy production while mostly preserving the simplicity of its design.

Theoretically predicting the performance of the SWT is difficult due to a large number of variables affecting its performance. The effect on performance us usually measured in either experimental or numerical studies. Experimental measurements usually include a wind tunnel which is used to measure the SWT performance on different wind conditions. Numerical methods use computational fluid dynamics (CFD) to measure the turbine on different conditions.

Theoretical ways to predict the performance of the SWT are difficult due to the nature of the airflow around it and the interference caused by the blades. Experimental ways to model the performance of the SWT are wind tunnel tests and field tests. Experimental studies provide reliable data on the behaviour of the SWT on different operating conditions. On the other hand, experimental tests are expensive and time-consuming to conduct with numerous different designs of the SWT. Multiple studies use numerical methods to supplement experimental results.

4.1 Factors affecting the performance of the Savonius wind turbine

Despite the simple basic design of the SWT, there are numerous different factors that affect its performance. Additionally, there are many different ways to improve the performance of the SWT with additional components. Performance affecting factors are covered specifically this section. Selecting the best parameters for optimal performance while

maintaining a relatively high efficiency is the goal of numerous experiments discussed in this section.

The blades of the SWT can also be modified significantly to affect the performance of the rotor. The number of blades can be increased from the original two-bladed SWT. The arc angle of the blade can have effect on the performance of the rotor. The blades can also be twisted. The number of stages can be increased. The aspect ratio of the SWT can be modified to change some performance related factors. Shape and dimensions of the blades can affect the performance significantly. The inclusion of turbine end plates seems to be standard among studies. Static parts can be added in front of the blades to affect the air flow to the blades. Overlap ratio and spacing between blades can be altered.

In addition, the characteristics of the flow affect the performance of the rotor. Since Reynolds number is important flow related quantity in fluid mechanics, its effect on SWT performance can be significant.

4.1.1 Number of blades

The basic design of the SWT includes two half cylindrical blades between end plates. In this section, the performance of the SWT is being evaluated between different number of blades. Increasing the number of blades on the SWT can decrease the power coefficient of the SWT. Increasing the area of the convex part of the blades increases the negative torque which reduces the total torque difference between blades. (Mercado-Colmenero et al., 2018)

Blackwell et al. studied the performance of multiple two- and three-bladed SWT variants. The three-bladed SWT had much less variation in static torque coefficient than the two-bladed variant. Excluding the starting torque, two-bladed variants had better performance overall. (Blackwell et al., 1977, p. 33)

The study by Roy and Saha came into a conclusion that two-bladed SWT has the best performance. Increasing the blade number to three increased the starting torque. Four-

bladed variant had the worst efficiency by far. According to the numerical study, two- and three-bladed rotor achieved power coefficients of 0.165 and 0.12 respectively. (Roy and Saha, 2013, p. 80)

The effect of the number of blades on the performance of the SWT was studied both experimentally and numerically by Wenehenubun et al. The experiment used a SWT with 2, 3 and 4 blades with an overlap ratio of 0.15 and aspect ratio of 1.0. Experimental setup included small open circuit wind tunnel and was measured with a low wind speed between 1 and 10 m/s. The SWT remained outside at the end of the wind tunnel during experiment. Results of the experiment show that the three-bladed SWT achieved the highest TSR while the four-bladed had the lowest. The results also indicated that the four-bladed SWT had the highest power coefficient while the two-bladed one had the lowest. The four-bladed SWT had the highest power coefficient at lowest TSR value, which indicates that the two-bladed variant could have the highest power coefficient at higher TSR. (Wenehenubun et al., 2015, pp. 301–302)

As a conclusion, most of the examined studies agree that the best power coefficient can be achieved with a two-bladed SWT. Adding more blades increases the starting torque and reduces the variance of the static torque. In addition, higher blade count can move the highest power coefficient to lower TSR values.

4.1.2 **End plates**

End plates are commonly used in SWTs. A SWT usually contains two round end plates placed above and below the rotor blades. A parameter often discussed in studies is the ratio between the diameter of the end plates and the diameter of the rotor. This ratio is referred to as the diameter ratio in this thesis. Inclusion of the end plates increases the performance of the SWT notably by preventing the air from flowing over and under the blades. This increases the pressure difference between convex and concave side of the blade considerably.

According to the study by Akwa et al., a diameter ratio of 1.1 would lead to highest power coefficient. For better performance on low wind speeds, thickness of end plates should be minimized. Higher diameter ratio can lead to increased rotor inertia. (Akwa et al., 2012, p. 3057)

Research has been done about the effect of end plates in SWT with multiple different turbine sizes by Jeon et al. Research studies the possibility of using partial end plates. Assuming the use of end plates increases the torque caused by the advancing blade, end plates also increase negative torque caused by returning blade. To reduce the amount of negative torque caused by the returning blade, different end plate designs that cover only parts inside the blade arc were studied. Using smaller end plates would also lead to less material usage, less building costs and lighter design. The research included subsonic wind tunnel tests in an open circuit. The experiment used four different sizes of the end plates with an aspect ratio of 2.0 and twist angle of 180°. Turbines had no overlap or separation between the blades. In addition, one turbine had ordinary circular end plates the same diameter as the blades. (Jeon et al., 2015, pp. 167–168)

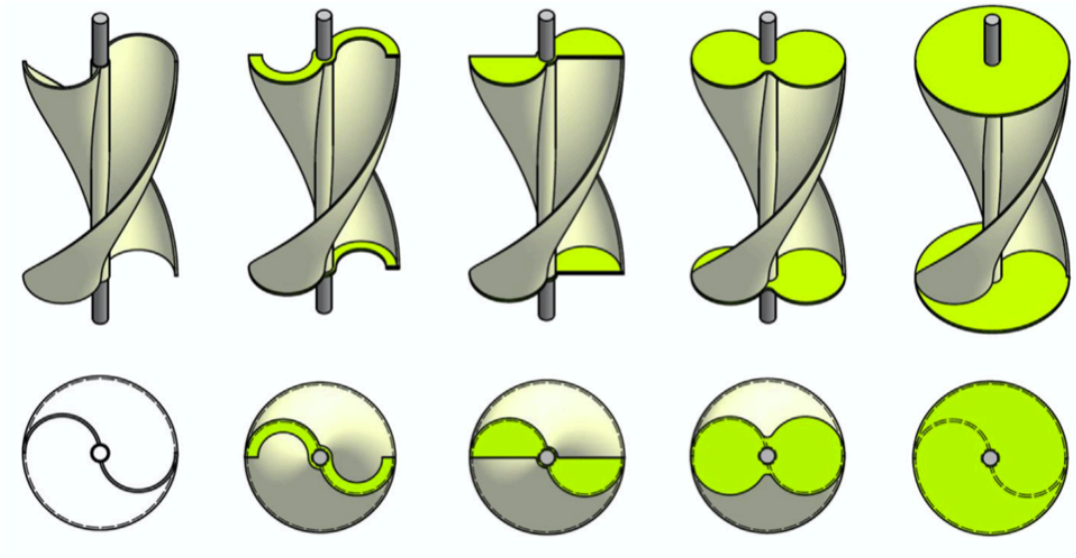

Figure 10. Twisted Savonius wind turbines with multiple different end plate designs. (Jeon et al., 2015, p. 169)

Research concluded with results that show linearly rising TSR. Lowest TSR value was measured with no end plates at all while highest value was achieved with circular end plates that had diameter ratio of 1.0. Percentage increase from the lowest power coefficient to the highest was 36 %. (Jeon et al., 2015, p. 175)

As a conclusion, the end plates increase the performance of a SWT notably, and the optimal diameter of the end plates is slightly larger than the diameter of the rotor. Other end plate designs than the conventional circle resulted in lower power coefficients.

4.1.3 **Blade arc angle**

Blade arc angle indicates how many degrees the arc of the turbine blade is. The most common design of the SWT has a semi-circular arc which means the blade arc angle is 180 degrees. Optimizing the blade arc angle is a simple potential way to increase the performance of a SWT. A SWT with blades with an arc angle of 180 degrees is shown in figure 7.

According to study by Mao and Tian, an arc angle of 160° results in higher power coefficient of 28.36. Power coefficient was higher than that of the ordinary turbine by 8.37 %. Results showed that by reducing the ellipticity of the blade the peak torque caused by the blade is increased. In addition, the negative torque caused by the returning blade is also reduced. The numerical simulations were compared to the existing experimental data which showed similar results that backed numerical data. (Mao and Tian, 2015, p. 1)

Simulations included tests with six different blade arc angles, 150°, 160°, 170°, 180°, 190° and 200°. The results indicated, that the torque rises when the blade arc angle is increased until 160°. The turbine tip–to–speed ratio also affected the results. A blade with an arc angle of 160° had the highest torque when the tip–to–speed ratio was over 1.2. Additionally, the torque was highest with the blade that had an arc angle of 170° with a tip–to–speed ratio of less than 1.2. Torque started clearly going down after 160–170°. (Mao and Tian, 2015, p. 7)

The experimental study by Kamoji et al. included blade arc angles of 100°, 124°, 135° and 150°. Tests were conducted with two Reynolds numbers of 120000 and 150000. The Highest power coefficient was achieved with an arc angle of 124°. Lower and higher arc angle achieved clearly lower performance with the worst being 150°. However, Kamoji et al. used a modified SWT design with a blade shape factor of 0.2. (Kamoji et al., 2009a, p. 1069)

Optimizing the blade arc angle gives varying results between studies. There are obviously other factors that affect the optimal arc angle of the blade such as shape of the blade. The effect on performance is considerable, so finding the optimal angle can be worthwhile depending on the turbine design.

4.1.4 **Twist**

Some SWTs have blades with a certain amount of twist. SWTs with twisted blades are referred to as helical turbines. The performance of multiple SWT variants with different twist angles and Reynolds numbers was studied by Lee et al. Reynolds numbers used in testing were $1.24 \cdot 10^6$ and $1.55 \cdot 10^6$. The study was executed with both CFD simulations and experimental setup. The twist angles varied between 0° and 135°. With tip–to–speed values also varying in testing, the highest power coefficient was always found, when TSR was within the range of 0.5 to 0.65. The results indicated that the most optimal twist angle for SWT was 45°. With twist angle at 45° and TSR at 0.54, power coefficient was as high as 0.13. Lowest power coefficient of 0.12 was recorded when TSR was 0.45 and twist angle was 135°. It was found that when twist angle was between 90° and 135°, power coefficient remained constant. Reported maximum error of uncertainty was 5 % at most. (Lee et al., 2016, p. 237)

Kamoji et al. tested the performance of helical SWT with a twist of 90° with two overlap ratios of 0.0 and 0.1. While the conventional SWT had negative areas on the static torque coefficient, the helical SWT had only positive static torque coefficients for all rotor angles. When compared to a conventional SWT, the power coefficient was similar on the helical SWT with an overlap ratio of 0.0. The helical variant with an overlap ratio of 0.1

achieved lower power coefficient. Additionally, the helical SWT achieved the highest power coefficient with lower TSR than the conventional SWT. Being able to operate at lower TSR leads to less problems related to vibrations. (Kamoji et al., 2009b, p. 528)

As a conclusion, adding twist to the blades of a SWT does not necessarily affect the power coefficient by a large margin. The advantages are more uniform static torque distribution and being able to operate at lower TSR.

4.1.5 Stator vanes and curtain plates

The SWT rotor can be included with stator vanes. Stator vanes are non-movable vanes added around the rotor to affect the flow. Another similar approach is curtain design where larger flow deflecting plates are added in front of the SWT as shown in the figure 11. The goal of the curtain plates is the same as that of the stator vanes.

There is a number of benefits when using stator vanes or other flow deflecting structures around the rotor. The flicker that turbine blades cause is reduced, as static blades are added to cover the visual access to the blades. Vanes can also improve the self-starting capabilities of the SWT. The vanes should also increase the performance of the rotor by accelerating and guiding the flow. The effect that vanes or other shielding structures have on the performance of the SWT are discussed in this section. Additionally, a study by Grönman et al. suggests that stator vanes may accelerate the air flow relatively more at lower rotational speeds. (Grönman et al., 2019, pp. 864–867)

Since a large part of the negative torque is caused by the convex side of the returning blade, the aerodynamic efficiency of the SWT could be improved with a better flow concentration on the concave side of the advancing blade. (Altan and Atılgan, 2012, p. 1493)

A Study by Akwa et al. reached similar conclusions. Stators can be used to increase performance of the SWT by guiding the flow into certain direction. Efficiency gains are achieved by reducing the negative moment caused by the returning blade. (Akwa et al., 2012, p. 3063)

The effect of curtain plates on a conventional SWT was studied numerically by Roy and Saha. As with the stator vanes, a clear increase in the static torque is noticeable (Roy and Saha, 2013, p. 80). Another numerical study by Altan and Atılgan tried to reduce the the negative torque on the convex side of the blades and accelerate the flow into the concave side. The study showed a clear increase of the torque on all rotor angles. The angle of the curtain also had a large impact on the torque. (Altan and Atılgan, 2010, pp. 825–826)

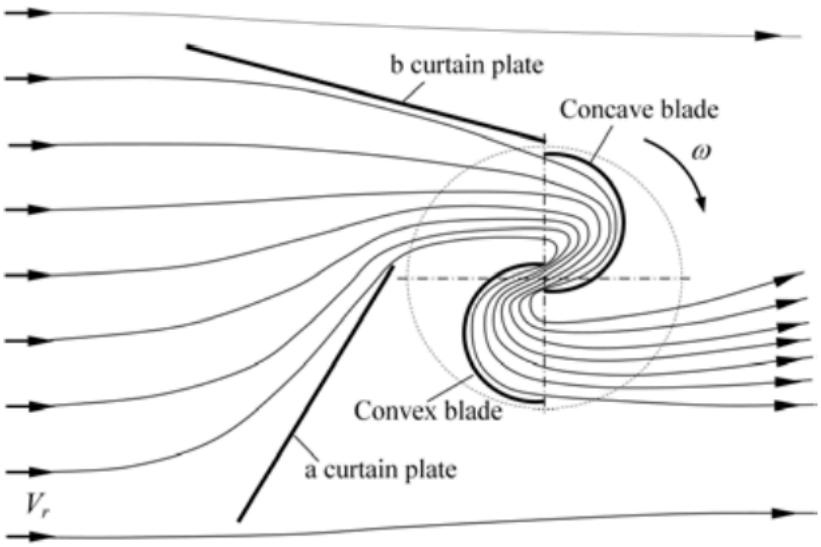

Figure 11. Savonius wind turbine with added curtain elements to concentrate flow into advancing blade. (Altan and Atılgan, 2012, p. 1494)

A clear consensus between studies is that flow deflecting structures can notably increase the performance of a SWT. The downside is that the weight and size of the turbine is increased. Additional vanes and plates also increase the building cost of the turbine.

4.1.6 **Number of stages**

Savonius wind turbine can be configured with additional stages. Stage means a set of rotor blades between two end plates. If a turbine contains multiple stages, the stages are stacked on top of each other.

According to the tests made in an open jet wind tunnel with one stage, two stage and three stage Savonius wind turbines, the single stage design was the most efficient of the three. Difference between two stage and three stage designs were negligible in terms of torque coefficient and power coefficient. All three designs feature the same rotor aspect ratio of 1.0. The blockage ratio used in this experiment was 28 %. A single stage SWT with an aspect ratio of 1.0 achieved maximum power coefficient of 0.18 at a tip–to–speed ratio of 0.7–0.8 and wind speeds of 10–12 m/s. Two stage SWT, which had a stage aspect ratio of 0.5 and rotor aspect ratio of 1.0 achieved peak power coefficient of 0.175 again at TSR of 0.7–0.8 with winds speed at 12 m/s. Three stage SWT with stage aspect ratio of 0.33 and a rotor aspect ratio of 1.0 achieved a peak power coefficient of 0.15 at TSR of 0.7–0.8 at a wind speed of 12 m/s. (Kamoji et al., 2008, pp. 893–894)

4.1.7 **Aspect ratio**

The aspect ratio of a SWT can be calculated by dividing the turbine height by its diameter. A high aspect ratio can reduce losses caused by the bucket tips. According to Akwa et al., the rotor efficiency increases as its aspect ratio increases. According to the study, an aspect ratio of 2.0 is high enough for most of the efficiency gains. As the turbine aspect ratio is increased, rotor moment and turbine inertia are decreased while angular acceleration is increased. Since the aspect ratio affects the turbine rotational speed, it can be modified to achieve the optimum rotation speed according to the needs of the turbine application. Compared rotors include models with no end plates, with end plates and with end plates and deflectors. (Akwa et al., 2012, pp. 3057–3058)

Kamoji et al. studied the effect of the aspect ratio on the SWT with Reynolds numbers 120000 and 150000. The aspect ratios studied were 0.6, 0.7, 0.77 and 1.0. An aspect ratio of 0.7 achieves highest power coefficient. It is noteworthy that Kamoji et al. used a modified SWT called the Bach rotor where blades have a straight part near the shaft. (Kamoji et al., 2009a, p. 1068)

Blackwell et al. studied the performance of SWT variants with heights being either 1.0 or 1.5 meters with same rotor diameters. Slightly better performance was achieved with higher aspect ratio. (Blackwell et al., 1977, p. 33)

Results for optimal aspect ratio vary quite a bit between studies and turbine models. Increasing the aspect ratio can increase the efficiency slightly at the cost of increasing turbine weight. Consensus seems to be that the aspect ratio can be used to modify turbine rotational speed and torque. In addition, a high aspect ratio may increase the power-to-weight ratio of the SWT (Mercado-Colmenero et al., 2018, p. 211).

4.1.8 **Overlap ratio**

Overlap ratio for the SWT is the ratio between the rotor blade overlap distance and the rotor diameter. Overlap distance is visualized in the figure 7. Since the overlap ratio affects the performance of the SWT, this section covers possible values for the optimal overlap ratio.

Study conducted by Rus et al. found out, that the optimal overlap ratio for the SWT is 0.3 when wind speed is between 0 m/s and 7 m/s. The SWT with an overlap ratio of 0.15 achieved average generated power of 0.61 W when wind speeds were between 0 m/s and 7 m/s. Mechanical power in the turbine was 1.8 W at the time which represented 25 % of total power available in wind. With higher overlap ratio of 0.3, average generated power at the same wind speed was 0.64 W with total turbine power at 1.97 W reaching 29 % of total mechanical energy in wind. According to the study, overlap ratio of 0.15 is preferred in areas, where wind speeds are constantly under 4 m/s. Differences in power generation are clearer at higher wind speeds. The generated power increases with higher overlap ratio when wind speed is 7 m/s. (Rus et al., 2018, p. 1798)

Kamoji et al. tested SWT performance with overlap ratios of 0.0, 0.10 and 0.16 with two Reynolds numbers of 120000 and 150000. The results indicate, that the one with no overlap ratio resulted in best performance with both Reynolds numbers. According to the

study, the aerodynamic performance of the SWT is reduced on higher overlap ratios than 0.15 due to losses caused by vorticities. (Kamoji et al., 2009a, pp. 1067–1068)

A study by Blackwell et al. came into a conclusion, that optimal overlap ratio is between 0.1 and 0.15 (Blackwell et al., 1977, p. 33)

Optimizing the overlap ratio for the SWT can bring small performance improvements with simple design changes. Optimizing the overlap ratio can be difficult due to the variation in the optimal overlap ratio with different wind velocities and varying testing environments. Since no specific value for optimal overlap ratio was found, a range to which most studies seem to end up can be stated. Study by Mercado-Colmenero et al. ends up with range between 0.15 and 0.3 (Mercado-Colmenero et al., 2018, p. 211). Another study by Zemamou et al. shows multiple studies leading to optimal overlap ratio between 0.1 and 0.3 (Zemamou et al., 2017, p. 386).

4.1.9 **Reynolds number**

Reynolds number is a dimensionless quantity that describes the nature of the flow. The performance of the SWT is influenced by the Reynolds number. The Reynolds number has an effect on the separation of the turbine layer on the blades of the turbine. As Reynolds number increases, separation of the boundary layer is delayed. (Akwa et al., 2012, p. 3062)

Experimental study by Grönman et al. studied the performance of a vaned SWT. The study indicates, that power coefficient of SWT decreases with lower Reynolds number values. Over 20 % drop in power coefficient was measured over the Reynolds number range. Decreasing Reynolds number could also move peak power coefficient into higher TSR values. (Grönman et al., 2019, p. 867)

According to a study by Kamoji et al., the highest power coefficient is achieved with the highest Reynolds number of 150000. Reynolds number values were between 80000 and

150000. It's also pointed out that higher power coefficient may be related to delayed separation of the boundary layer on higher wind velocities. The tests were conducted with a modified SWT with an overlap ratio of 0.7, blade arc angle of 124°, blade shape factor of 0.2 and end plate ratio of 1.1. (Kamoji et al., 2009a, p. 1069)

Another study by Kamoji et al. studied the performance of a helical SWT. Reynolds numbers varied between 57700 and 202000 while wind velocities were between 4 m/s and 14 m/s. The results indicate, that higher Reynolds numbers lead to higher performance. The highest power coefficient of 0.2 was achieved with Reynolds number 202000. (Kamoji et al., 2009b, p. 525)

Blackwell et al. came into a conclusion, that Reynolds number generally increases the performance of the SWT. The study used two Reynolds numbers of around 432000 and 867000. (Blackwell et al., 1977, p. 33)

A clear consensus is that increasing Reynolds number raises the power coefficient curve of the wind turbine. The increase in power coefficient seems to be related to later boundary layer separation.

4.1.10 **Other factors**

Blade shape factor applies only to SWTs where blade is not only circular but includes straight part near the turbine shaft. The blade shape factor is defined as the ratio of straight part of the blade to the radius of blade arc. Experimental study by Kamoji et al. included performance tests on the SWT with three different blade shape factors of 0.2, 0.4 and 0.6 over two Reynolds numbers of 120000 and 150000 (Kamoji et al., 2009a, p. 1069). The study achieved the highest power coefficient with a blade shape factor of 0.2 by a small margin. More experimental data with comparison to a conventional SWT is needed in order to draw any conclusions on the blade shape factor. The blade shape factor does not seem to affect the performance by a significant amount.

Spacing in the SWT means the space between blades perpendicular to the overlap space. Large spacing between blades reduces performance of the SWT by leading air away from concave side of the blade. Best performance seems to be achieved with zero spacing. (Akwa et al., 2012, p. 3058)

4.2 Correlation for Savonius wind turbine performance

This section explores the existence of a possible performance-related correlation for SWT. Multiple studies have hinted at a Reynolds number dependent correlation for a torque coefficient of a SWT. The correlation for the performance of the SWT uses torque coefficient, Reynolds number and tip–to–speed ratio. Since different variations of said correlation have been found, reasons for this discovery and differences between studies are being sought.

Multiple studies have researched the correlation, where torque coefficient divided by Reynolds number to power n. The correlation found in the studies has been either first or second order polynomial function. A correlation found by Mercado-Colmenero et al. is shown in the following equation.

$$\frac{C_t}{Re^n} = p_1 \cdot \lambda^2 + p_2 \cdot \lambda + p_3 \quad (6)$$

n is dimensionless factor

p_n is factor for tip–to–speed ratio

The correlation is interpolated from a curve against tip–to–speed ratio as a second order polynomial function. (Mercado-Colmenero et al., 2018, pp. 228–230)

In addition to a conventional SWT, the study used three different SWT variants with a varying twist angle. The correlation for variants with a twist angle of 0° and 45° used torque coefficients where Reynolds number was over 99070. The variant with a twist angle of 22.5° used torque coefficients where Reynolds number was over 71370. The removal of lower Reynolds numbers was due to distortion caused by viscous stresses

caused by the boundary layer. The study compared experimental values against those from numerical studies and correlation equation. The comparison resulted in maximum error of 3.5 %.

Kamoji et al. also studied the performance related correlation with modified single stage SWT. The modified rotor had no shaft between the end plates. Other dimensions include an aspect ratio of 0.7, an overlap ratio of 0, a blade arc angle of 124°, a blade shape factor of 0.2 and end plate ratio of 1.1. The test gathered torque coefficient over Reynolds numbers 77600, 103000, 129000 and 155000. Torque coefficients were used with the correlation term Ct/Re^n, where n was 0.3. The values of the term resulted into one single curve against TSR as opposed to more scattered torque coefficient values due to varying Reynolds number. The correlation achieved an error of less ±5 % with TSR being less than 1.0, when compared against the results from the experimental study. The study resulted in following linear correlation equation, which applies for aforementioned Reynolds numbers and for TSR of over 0.6. (Kamoji et al., 2009a, pp. 1071–1073)

$$\frac{C_t}{Re^{0.3}} = -0.0107 \cdot \lambda + 0.0149 \quad (7)$$

Kamoji et al. also studied the correlation on different study with helical bladed SWT. The rotor had an aspect ratio of 0.88, an overlap ratio of 0.0 and blades had a 90-degree twist. Torque coefficients that were used with the correlation term were measured with Reynolds numbers 86600, 100000, 115400, 120000, 144300, 173100 and 202000. Similar to the previous study by Kamoji et al., values from the correlation formed almost a single curve against TSR. The study achieved the following linear correlation equation with an error of ±6 %. Additionally, the correlation was used to calculate torque coefficients and power coefficients which resulted in an error of ±5 % when compared against experimental results. Study included measurements for Reynolds number values between 86600 and 202000 (Kamoji et al., 2009b, p. 528)

$$\frac{C_t}{Re^{0.3}} = -0.0128 \cdot \lambda + 0.0162 \quad (8)$$

Unlike the correlation from the study by Mercado-Colmenero et al., both correlations achieved by Kamoji et al. feature a linear correlation equation.

An experimental study by Grönman et al. studied the performance of a vaned SWT with three blades. The study also used the same first term of the of the correlation as initial condition. Following equation was achieved.

$$\frac{C_t}{Re^{0.27}} = 0.0231 \cdot \lambda^2 - 0.0459 \cdot \lambda + 0.0235 \quad (9)$$

This correlation is a polynomial equation such as one found out by Mercado-colmenero et al. It's notable, that this correlation was developed from measuring torque with Reynolds numbers varying between 221600 and 886300, which is a lot higher range when compared with studies by Kamoji et al. Values of TSR for measurements were between 0.39 and 0.94. Most of the measured data was found out to be under 5 % error around the correlation curve. (Grönman et al., 2019, p. 868)

The study compared the results with two turbines from an aforementioned study by Mercado-Colmenero et al. Since the study by Mercado-Colmenero et al. featured similar second-order correlation with much lower Reynolds numbers, it was concluded that Reynolds number does not explain the difference in the shape of the correlation when compared to the aforementioned studies by Kamoji et al. The study by Blackwell et al. was also compared against, since it features Reynolds numbers in the range of 432000 and 867000 (Blackwell et al., 1977). After applying the data for the first term of the correlation, a linear curve shape was revealed, which confirms that the shape is not explained by higher Reynolds number. (Grönman et al., 2019, p. 868)

Using C_T/Re^n as the initial condition for the correlation, other studies can be examined. Since the correlation depends on Reynolds number, studies that measure the torque with multiple different Reynolds numbers are preferred. This topic is discussed further in the next section, where previously mentioned studies and some additional are examined with the first term of the equation 7 as the initial condition.

5 WIND TURBINE PERFORMANCE MEASUREMENTS

To evaluate and compare the data between multiple experimental studies and factors, data has been gathered from those studies into one large file. The data was collected using an open source, non-commercial program called Engauge Digitizer. Only the tables with torque coefficients against tip–to–speed ratio were collected. Since data was collected manually from graphs, some mostly negligible inaccuracies will occur. Due to the amount of data collected, effect of inaccuracy is small.

Experimental data is gathered from studies presented in this section. Grönman et al. studied the effect of Reynolds number on SWT power coefficient and torque coefficient (Grönman et al., 2019, p. 867). Mercado-Colmenero et al. also studied performance of SWT with different Reynolds numbers (Mercado-Colmenero et al., 2018, pp. 220–223). Kamoji et al. studied the SWT performance on different conditions comprehensively (Kamoji et al., 2009a). The experiments included the effect of overlap ratio, aspect ratio, blade arc angle and blade shape factor on different SWT designs over multiple Reynolds number values. Kamoji et al. also studied the effect of blockage ratio, stage aspect ratio and rotor aspect ratio on different Reynolds number values for single stage, two stage and three stage Savonius wind turbines (Kamoji et al., 2008). El-Askary et al. studied the SWT performance on different blade twist angles. The effect of twist angle is taken into account (El-Askary et al., 2018, p. 350). Damak et al. studied the performance of a helical SWT and a helical SWT combined with a Bach rotor with wind tunnel experiments (Damak et al., 2018). Blackwell et al. studied the performance of multiple conventional SWT models with some changes in basic dimensions (Blackwell et al., 1977). Figure 12 shows an example case about data collection using Engauge Digitizer and a figure form the study by Damak et al.

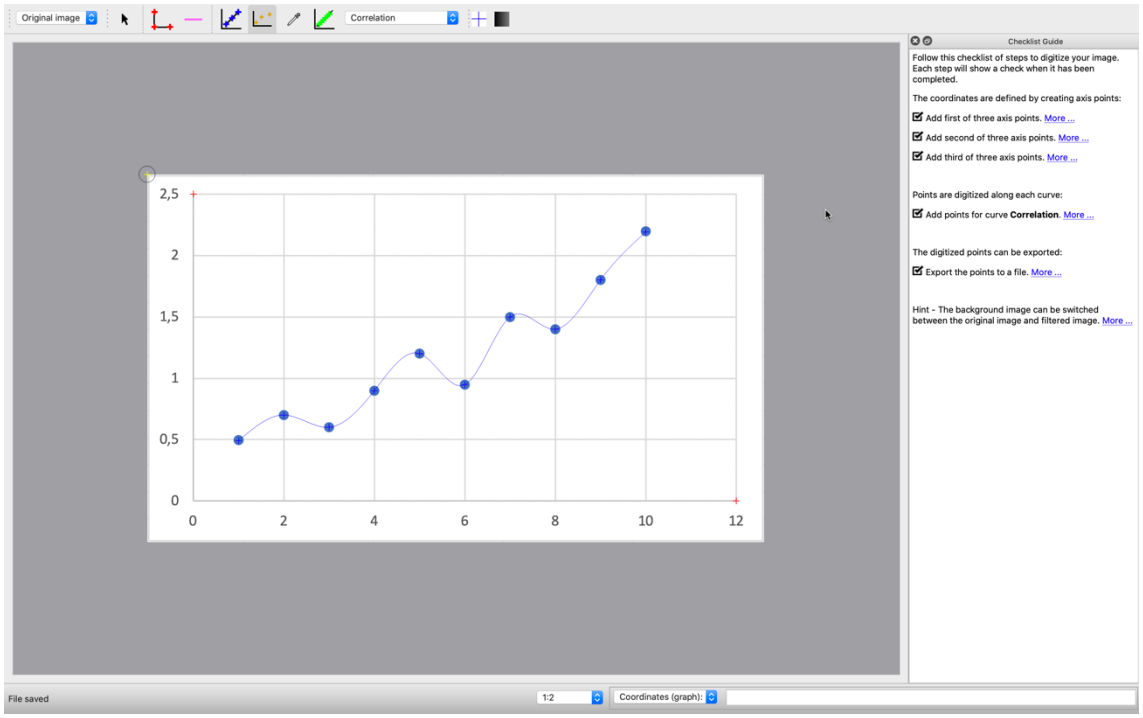

Figure 12. An example of data collection using Engauge Digitizer and example data.

5.1 Data from wind tunnel experiments

In this section, the data from wind tunnel experiments is reviewed systematically to find out how different design parameters affect the shape of the torque coefficient correlation and how they affect some variables of the correlation.

Wind tunnel data is gathered from experimental studies with different SWT variants. To study the shape of a possible correlation, experiments that measure torque coefficients over various Reynolds number values are needed. Due to limited amount of experimental data available, any tests that include more than one Reynolds number are investigated.

Data that contains torque coefficient against TSR is collected manually from experimental studies. Torque coefficient is then divided by corresponding Reynolds number that is raised to the power of n. Exponent n is used in the performance correlation by multiple studies and usually has a value of around 0.3.

Basic dimensions and other typical design parameters are presented for each turbine which helps in finding how those parameters affect the results. Some of the design parameters were not present in all of the studies, so they were determined using other parameters. Overlap ratio has to be calculated differently when increasing the number of blades from two. In this section, overlap distance for rotors with three blades is the distance measure from the inner edge of the blade to the axis of the rotor as has been done previously in the study by Blackwell et al. (Blackwell et al., 1977).

Some of the studied experiments only measured torque after TSR of 0.4 to 0.6. To make results more comparable, some of the torque coefficients were removed when TSR was under 0.5 mainly from studies by Blackwell et al., Damak et al. and Kamoji et al. Most of the torque coefficient data points were more scattered at low TSR. The study by Grönman et al. had measured torque when TSR was over 0.39. The study by Colmenero et al. had torque values when TSR was over 0.1. The results from those two studies showed some relatively clear results even with lower TSR values.

A total of 52 figures all with slightly different turbine configurations were analysed from different studies for this thesis. Data was first gathered with Engauge Digitizer to be analysed in Microsoft Excel. Data was then fit into the initial condition of the correlation equation for the polynomial curve with correlation exponent originally as 0.3. The same thing was then done for the linear curve. To achieve enough data on multiple Reynolds numbers, data is combined from figures where the same turbine configurations are tested on multiple Reynolds numbers on different figures. This is indicated in the appendix I by showing multiple studied figures for one examined configuration.

After gathering the data, the coefficient of determination (R^2) was calculated for both linear and polynomial cases. Coefficient of determination indicates how near data points fall within the formed correlation curve. Coefficient of determination varies between 0 and 1 (0 % and 100 %). In other words, the higher the coefficient of determination is, the better the formed correlation curve fits the experimental data. To find out, whether linear

of polynomial curve is better suited for the figure, optimal value of the correlation equation exponent for both the polynomial and linear equation were required. The optimal value of the exponent is sought by using the Microsoft Excel add-in Solver. Solver is used to find what correlation exponent results in the highest coefficient of determination for both linear and polynomial correlation curves.

5.1.1 A SWT with stator vanes by Grönman et al.

Grönman et al. studied the performance of a SWT with stator vanes over seven Reynolds numbers and multiple different TSR values. Tests are conducted experimentally with wind tunnel. The experimental setup used in the study included a SWT with three blades with additional stator vanes around the rotor. Table 2 shows some basic dimensions of the studied SWT. Vane dimensions are not covered in detail in this table since no other suitable experimental studies about SWTs with stator vanes were found. (Grönman et al., 2019)

Table 2. Basic dimensions and measurement values of the helical rotor (Grönman et al., 2019).

Rotor diameter	d	[m]	0.580
Rotor height	h	[m]	0.300
Rotor aspect ratio	h/d	[-]	0.52
Rotor overlap ratio	o	[-]	0.175
Number of blades	n_b	[-]	3
Number of stages	n_s	[-]	1
Tip–to–speed ratio	λ	[-]	0.39–0.94
Reynolds number	Re	[-]	221600–886300

The goal of using vanes was to guide the flow into the advancing blade of the rotor and reduce the amount of flow going against the returning blade at the same time. Turbine

performance was measured using Göttingen-type closed-loop wind tunnel. To measure the effect of stator-rotor interaction, all tests were also conducted with stator only.

Measurement data was used to form a correlation for the turbine performance. Results were compared to experimental studies by Kamoji et al. and Colmenero et al., which are also analysed in later sections.

Experimental data was collected from the study to compare it to the results of other experimental studies. Data that shows measured data with seven different Reynolds numbers is visible in figure 13(a). When the experimental data is used with the initial condition to the correlation, a clear room for second order correlation can be detected as explained in study. The correlation curve is shown in the figure 13(b). Correlation that was formed in the same study with the initial condition being c_t/Re^n is displayed in the same figure. An exponent of approximately 0.273 was used in the correlation equation which resulted in the highest coefficient of determination. Due to slightly different exponent and small differences from the data collection method, the formed correlation equation is slightly different from the one found in the original study. The formed correlation curve is shown in following equation. (Grönman et al., 2019, p. 868)

$$\frac{C_T}{Re^{0.273}} = 0.0222 \cdot \lambda^2 + 0.0443 \cdot \lambda + 0.0227 \quad (10)$$

(a) (b)

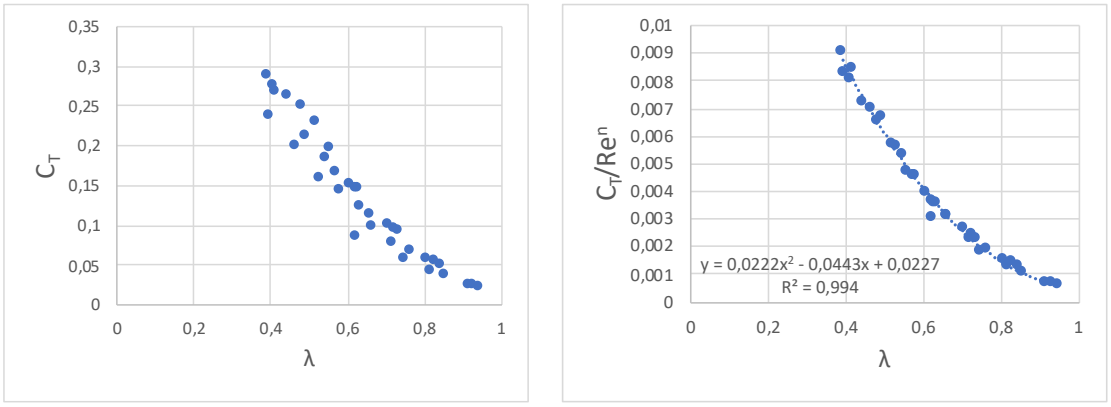

Figure 13. Torque coefficient data (a) and data where c_t/Re^n is used as initial dependency (b) from the experimental study. A correlation exponent of approximately 0.273 was used which resulted in the best coefficient of determination of 0.994 as shown in the figure. (Grönman et al., 2019, pp. 867–868, fig. 3a-5a)

5.1.2 SWTs with varying stage numbers by Kamoji et al.

Kamoji et al. studied the performance of five different SWT variants. Variants included turbines with one, two and three stages. Ranges for basic design parameters are in table 3. The variant with one stage had a rotor aspect ratio of 1.0. Two variants with two stages were tested with stage aspect ratios of 1.0 and 0.5 while rotor aspect ratios were 1.0 and 0.5 respectively. Two of the three-stage variants had stage aspect ratios of 0.33 and 1.0 while rotor aspect ratios were 1.0 and 3.0. Performance measurements included tests with multiple Reynolds numbers. The basic dimension ranges for the turbine models are shown in the table 3. (Kamoji et al., 2008, p. 877)

Table 3. Basic dimension ranges with Reynolds numbers and tip–to–speed ratios used in this analysis for five SWT variants (Kamoji et al., 2008).

Rotor diameter	d	[m]	0.0966–0.225
Rotor height	h	[m]	0.208–0.2899
Rotor aspect ratio	h/d	[-]	1.0–3.0
Rotor overlap ratio	o	[-]	0.15

Number of blades	n_b	[-]	2
Number of stages	n_s	[-]	1–3
Tip–to–speed ratio	λ	[-]	0.5–1.4
Reynolds number	Re	[-]	36000–168000

The performance of a single-stage SWT with a blockage ratio of 28 % is shown in figure 14. Tests were carried out with Reynolds numbers 77600, 103500, 129500 and 155000 with wind speeds of 6, 8, 10 and 12 m/s respectively. Figure 14(a) shows torque coefficients as a function of the TSR. Figure 14(b) shows the optimal linear correlation curve for the single-stage SWT. The optimal value for the exponent of the correlation equation was found to be approximately 0.208 for the linear curve. The linear curve leads to a coefficient of determination of 0.982. Data points from the correlation equation are clearly less scattered when compared to data points from torque coefficients. The data seems to fit the correlation curve best when TSR is between 0.6 and 1.0. The following equation shows the correlation curve achieved with previously mentioned values.

$$\frac{C_T}{Re^{0.208}} = -0.0294 \cdot \lambda + 0.0415 \tag{11}$$

(a) (b)

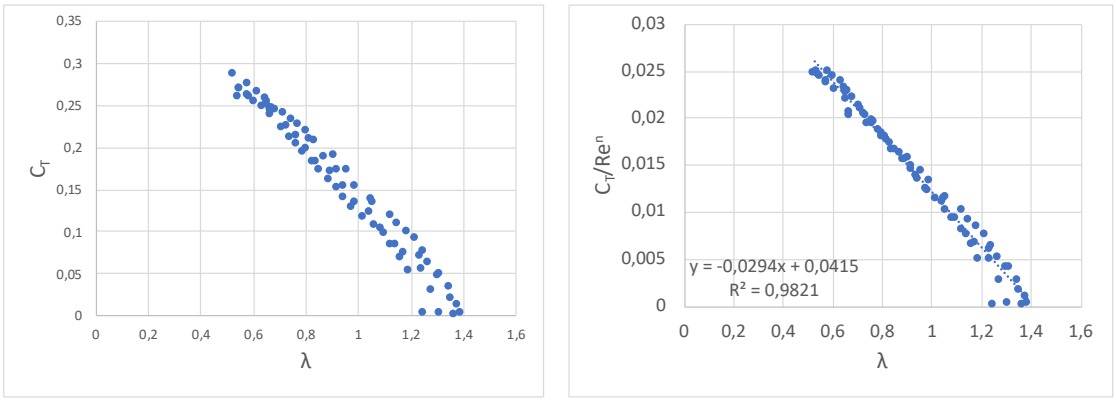

Figure 14. Performance of a single-stage SWT as a function of tip–to–speed ratio. Figure (a) shows torque coefficient values against TSR. Figure (b) shows the linear correlation curve. The

optimal correlation exponent used in the figure (b) is approximately 0.208. Data is collected from an experimental study (Kamoji et al., 2008, p. 882, fig. 5).

Figure 15 shows the performance of a two-stage SWT with a rotor aspect ratio of 1.0. The measured torque coefficients are in the figure 15(a). Torque was measured within Reynolds numbers 84500, 112500, 140500 and 168500. Figure 15(b) shows the optimal linear correlation curve for the same rotor. Even better correlation could be achieved if TSR was limited to over 0.6 only, since data points start to turn downwards when TSR is under 0.6. The correlation curve was achieved with a correlation exponent of 0.147 which resulted in coefficient of determination of 0.978. A following equation was formed from the initial condition of the correlation.

$$\frac{C_T}{Re^{0.147}} = -0.0556 \cdot \lambda + 0.0775 \tag{12}$$

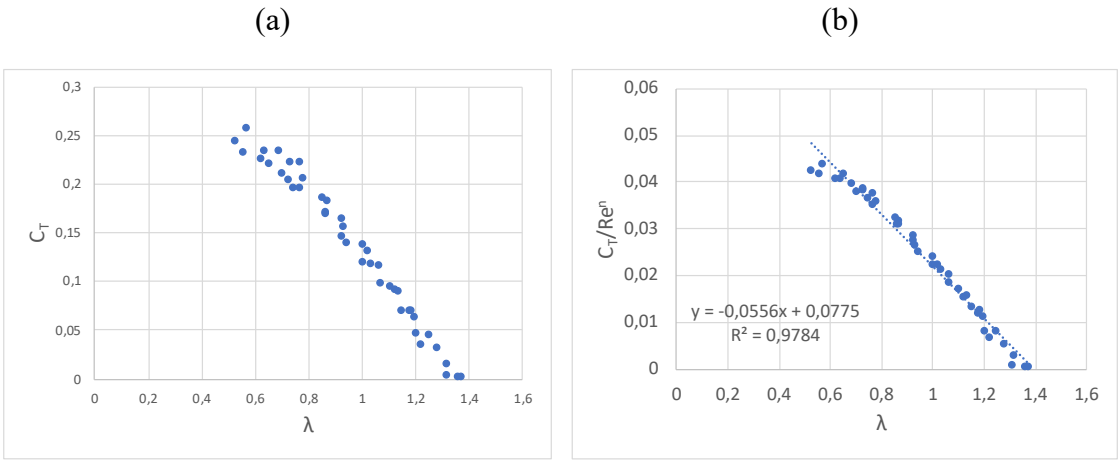

Figure 15. The performance of a two-stage SWT with a rotor aspect ratio of 1.0. Figure (a) shows measured torque coefficients while figure (b) shows the linear correlation curve. Correlation exponent of n = 0.147 was found to be the optimal value for coefficient of determination. Data is collected from an experimental study (Kamoji et al., 2008, p. 884, fig. 7).

Figure 16 shows the performance of a three-stage SWT with a rotor aspect ratio of 1.0. Measured torque coefficients are shown on the figure 16(a). Turbine torque was measured

over four different Reynolds number of 84000, 112000, 140000 and 168000. Figure 16(b) shows the formed correlation curve for the same turbine. The optimal correlation exponent used with the torque coefficient data was 0.255 which leads to a coefficient of determination of 0.982. The formed correlation clearly seems to be linear although the torque starts to turn down a little bit below the TSR of 0.6. The following equation was formed from the data.

$$\frac{C_T}{Re^{0.255}} = -0.0165 \cdot \lambda + 0.0211 \tag{13}$$

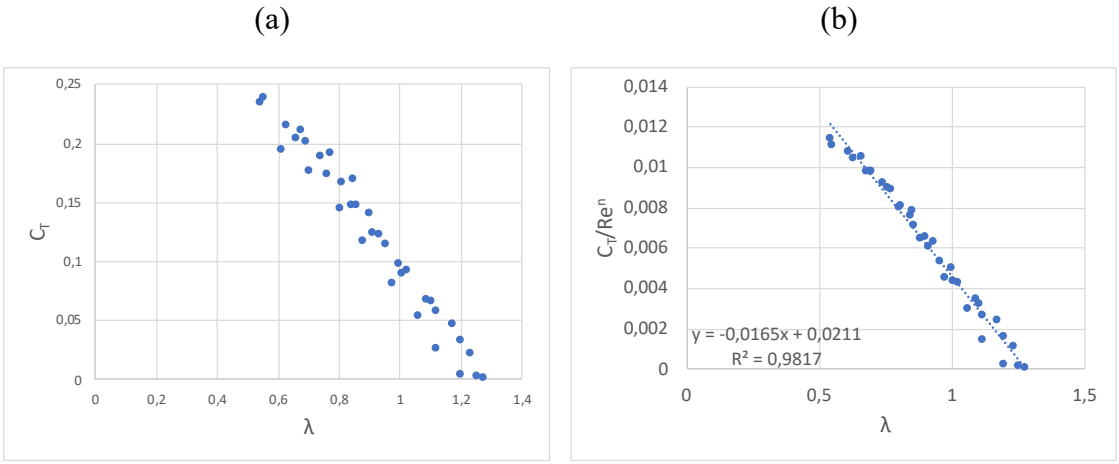

Figure 16. The performance of three-stage SWT with stage a rotor aspect ratio of 1.0. Figure (a) shows the torque coefficients while figure (b) shows the linear correlation curve. The optimal exponent of the correlation curve was found to be 0.255. Data is collected from an experimental study (Kamoji et al., 2008, pp. 887–888, fig. 10-11).

The study also included different variants for two- and three-stage rotors with rotor aspect ratios of 2.0 and 3.0 respectively. These two figures were measured with lower Reynolds numbers. Since a high aspect ratio of a rotor leads to a higher rotational speed on the same wind velocity, TSR range is similar to the previous cases with rotor aspect ratios of 1.0. These cases are not presented in this chapter. Results of the other cases can be seen in the appendix I. Lower Reynolds number range seems to result in more scattered results. Op-

timal linear correlations for two- and three-stage rotors achieved coefficients of determination of approximately 0.85 and 0.95, which are clearly lower than those of the other rotors examined in this section. The optimal correlation exponents were also clearly higher for the rotors with higher rotor aspect ratio. The highest linear correlation exponent was 0.708 when aspect ratio was 3.0 while the second highest exponent was 0.381 when aspect ratio was 2.0. Variants with an aspect ratio of 1.0 had optimal linear correlation exponents between 0.147 and 0.255.

5.1.3 **Modified SWT variants by Kamoji et al.**

In another experimental study carried out by Kamoji et al., the performance of modified conventional SWT is measured in wind tunnel tests to improve the power coefficient and uniform static torque coefficient. Tests are carried out with and without central shaft in the turbine. The experiment included tests with various different SWT parameters including aspect ratio, overlap ratio, blade arc angle, blade shape factor and Reynolds number. Study also included correlation for modified Single stage SWT verified with multiple Reynolds number values. The dimension ranges between the turbine models used in the study are visible in the table 4. (Kamoji et al., 2009a, p. 1064)

Table 4. Basic dimension ranges with Reynolds numbers and tip–to–speed ratios used in this analysis for modified SWT variants (Kamoji et al., 2009a).

Rotor diameter	d	[m]	0.180–0.230
Rotor height	h	[m]	0.126–0.230
Rotor aspect ratio	h/d	[-]	0.6–1.0
Rotor overlap ratio	o	[-]	0.1–0.16
Number of blades	n_b	[-]	2
Number of stages	n_s	[-]	1
Tip–to–speed ratio	λ	[-]	0.5–1.56
Reynolds number	Re	[-]	77600–150000

Tests were carried out with open-jet-type wind tunnel with square 400 mm * 400 mm outlet. Turbine is placed at 750 mm distance from tunnel outlet at the centre both horizontally and vertically. Most of the tests are carried out with Reynolds numbers 120000 and 150000. (Kamoji et al., 2009a, p. 1065)

The study contains numerous different SWT configurations with different aspect ratios, blade shape factors, blade arc angles and overlap ratios. Data from a total of 19 different configurations was collected and analysed. Most of the figures from the study contain torque coefficient data over two different Reynolds numbers of 120000 and 150000. Those with more data points over more Reynolds numbers are analysed in more detail. The behaviour of the torque coefficient data is once again examined when the TSR is greater than 0.5.

Figure 17 shows the effect of Reynolds number of the performance of a SWT with an aspect ratio of 0.2, an overlap ratio of 0, bladed arc angle of 124° and blade shape factor of 0.2. Torque coefficient data is in the figure 17(a) and the formed linear correlation is in figure 17(b). Torque coefficients were measured over Reynolds numbers 80000, 100000, 120000 and 150000. The linear correlation was formed with an optimal exponent of 0.329. The optimal linear correlation curve achieved a coefficient of determination of 0.978. The polynomial correlation did not achieve much higher coefficient. The performance of the stall and left the linear curve when TSR was under 0.5. A following equation was formed with the initial condition of the correlation equation.

$$\frac{C_T}{Re^{0.329}} = -0.0112 \cdot \lambda + 0.0136 \qquad (14)$$

(a) (b)

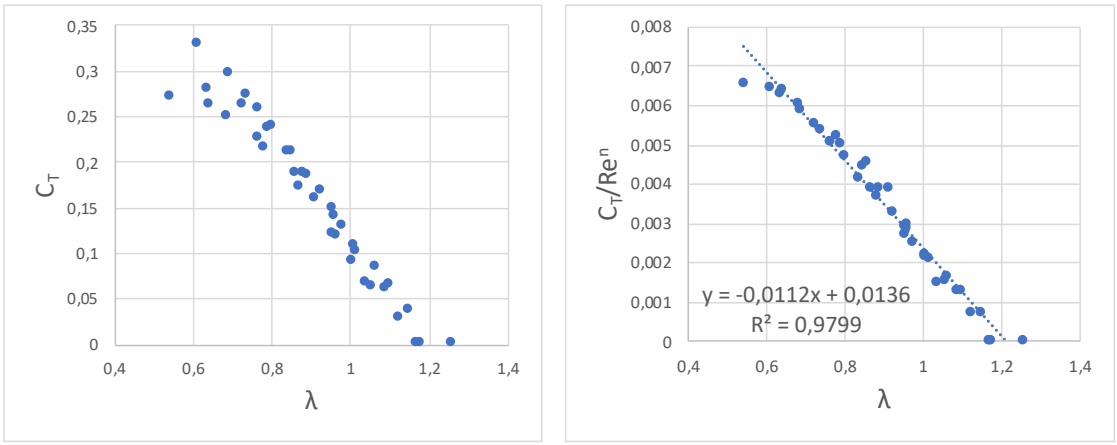

Figure 17. Torque coefficients (a) and a linear correlation curve (b) for a SWT with an overlap ratio of 0, an aspect ratio of 0.2, a blade arc angle of 124° and a blade shape factor of 0.2. The optimal correlation exponent was found to be 0,308 for the linear correlation. Data is collected from an experimental study (Kamoji et al., 2009a, p. 1071, fig. 14)

Figure 18 shows the experimental torque coefficient values fit into the initial condition of the correlation for a modified single stage SWT with an aspect ratio of 0.7 and an overlap ratio of 0.0. Multiple Reynolds numbers were used in the experiment with values being between 77600 and 150000.

Torque coefficients from the experimental study are in figure 18(a) and formed linear correlation in figure 18(b). Reynolds numbers were not differentiated in any way in the figure from the study, so an exponent provided by the study is used in the correlation. The exponent used in the study was 0.28. A coefficient of determination of 0.986 was achieved by using this exponent. The following equation was achieved with the exponent from the study.

$$\frac{C_T}{Re^{0.280}} = -0.0186 \cdot \lambda + 0.0233 \qquad (15)$$

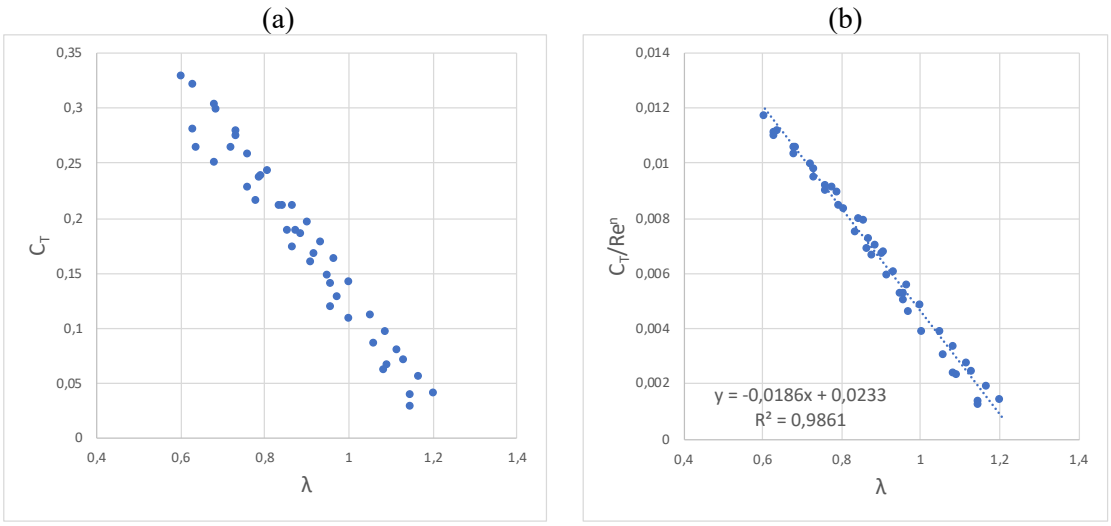

Figure 18. Torque coefficients from experimental study on a single stage modified SWT (a) and formed linear correlation curve (b). The SWT has an aspect ratio of 0.7 and overlap ratio of 0.0. Reynolds number values vary between 77600 and 150000. The optimal correlation exponent was found to be 0,280. Data is collected from an experimental study (Kamoji et al., 2009a, pp. 1072–1073, fig. 18-19)

In addition, the performance of conventional SWT (a) and modified SWT both with (b) and without (c) the shaft was compared in figure 19. Somewhat similar linear correlation equations were achieved, although the modified variant without shaft used higher correlation exponent of 0.426. All of the correlations achieved a relatively high coefficients of determination of around 0.98. The correlation equations are displayed in the figures but are not analysed further due to similarities with previous equations in this section.

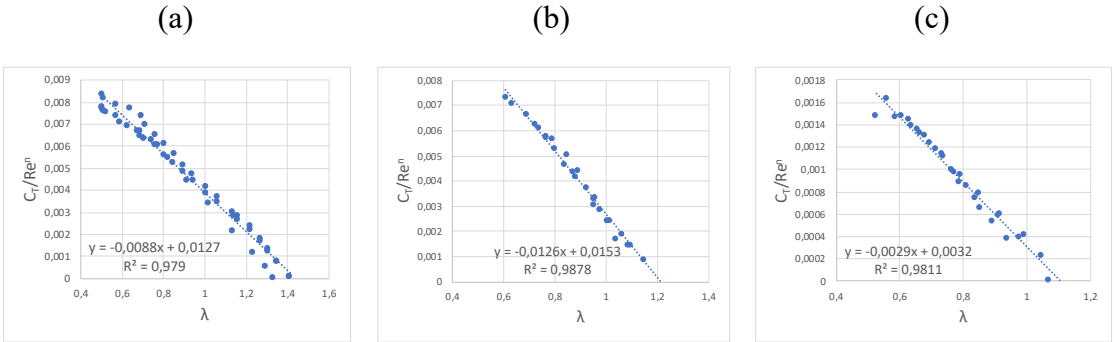

Figure 19. Correlation curve comparison of a conventional SWT (a), a modified SWT with shaft (b) and a modified SWT without a shaft (c). All of the curves are linear correlations formed with

optimal exponents of 0.302 (a), 0.319 (b) and 0.426 (c). Data is collected from an experimental study (Kamoji et al., 2009a, p. 1072, fig. 16).

Other figures included experiments on the effect of overlap ratio, aspect ratio, blade arc angle and blade shape factor. No large difference in the correlation equations were discovered. Correlation exponents were between 0 and 0.744.

5.1.4 Helical SWT variants by Kamoji et al.

Kamoji et al. also studied the performance of multiple variants of helical SWT. Blades of helical SWT are twisted by a certain angle. Twist is added to make torque more even throughout the turbine rotation. While conventional SWT has high static torque on some rotor angles, some other angles cause negative torque to the shaft. Twisted rotor blades used in the experiment have 90-degree twist. Table 5 shows some basic dimensions for the helical rotor. (Kamoji et al., 2009b)

Table 5. Basic dimensions with Reynolds numbers and tip–to–speed ratios used in this analysis for the helical rotors (Kamoji et al., 2009b)

Rotor diameter	d	[m]	0.211–0.230
Rotor height	h	[m]	202.4–253.2
Rotor aspect ratio	h/d	[-]	0.88–1.2
Rotor overlap ratio	o	[-]	0.0–0.16
Number of blades	n_b	[-]	2
Number of stages	n_s	[-]	1
Tip–to–speed ratio	λ	[-]	0.5–1.45
Reynolds number	Re	[-]	57702–201958

Figure 20 shows the effect of overlap ratio and aspect ratio on the correlation curve of multiple helical SWT variants. Figure 20(a) shows the performance of SWT with central shaft, overlap ratio of 0.0 and aspect ratio of 1.0. No enough data for a correlation of any kind can be detected. Rest of the variants had no central shaft and aspect ratios of 0.88 (b), 0.96 (c) and 1.0 (d). Optimal correlation exponents were between 0.47–0.8 for linear correlations. While somewhat similar on all variants, the exponents were still far from the mean exponent of around 0.27.

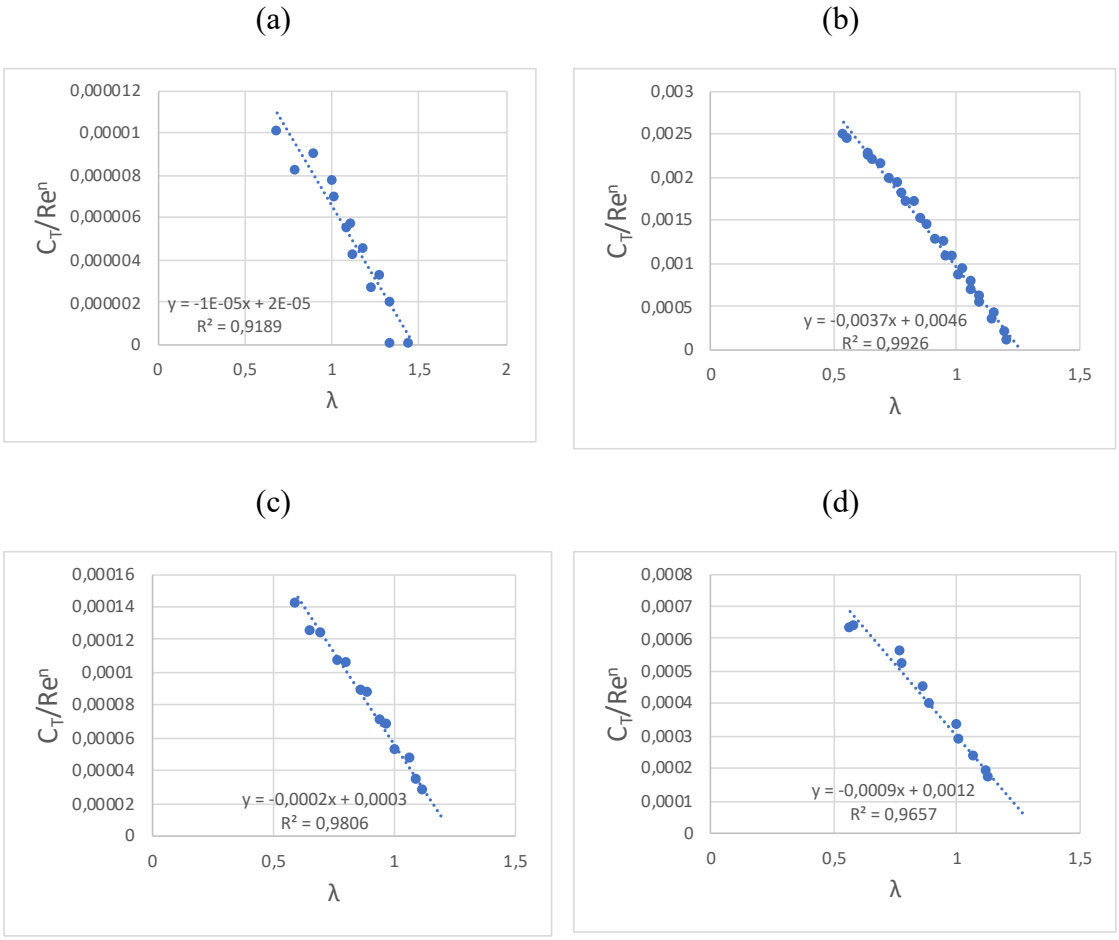

Figure 20. Correlation curves for four different SWT variants. Only the first variant (a) has a central shaft and an aspect ratio of 1.0. The rest had no central shaft and an aspect ratio of 0.88 (b), 0.96 (c) and 1.0 (d). Optimal linear correlation exponents were 0.799 (a), 0.402 (b), 0.617 (c) and 0.474 (d). Data is collected from an experimental study (Kamoji et al., 2009b, pp. 524–526, fig. 5-6).

Figure 21 shows the performance of helical SWT on Reynolds number values 57702, 86554, 115405, 144256, 173107 and 201958 with respective wind velocities being 4, 6, 8, 10, 12 and 14 m/s respectively. Rotor has a twist of 90 degrees, an aspect ratio of 0.88 and an overlap ratio of 0.0. Torque coefficients measured in the experimental study are presented in figure 21(a). Figure 21(b) shows the linear correlation curve formed from the experimental data with a correlation exponent of 0.446. The correlation achieved a coefficient of determination of 0.981.

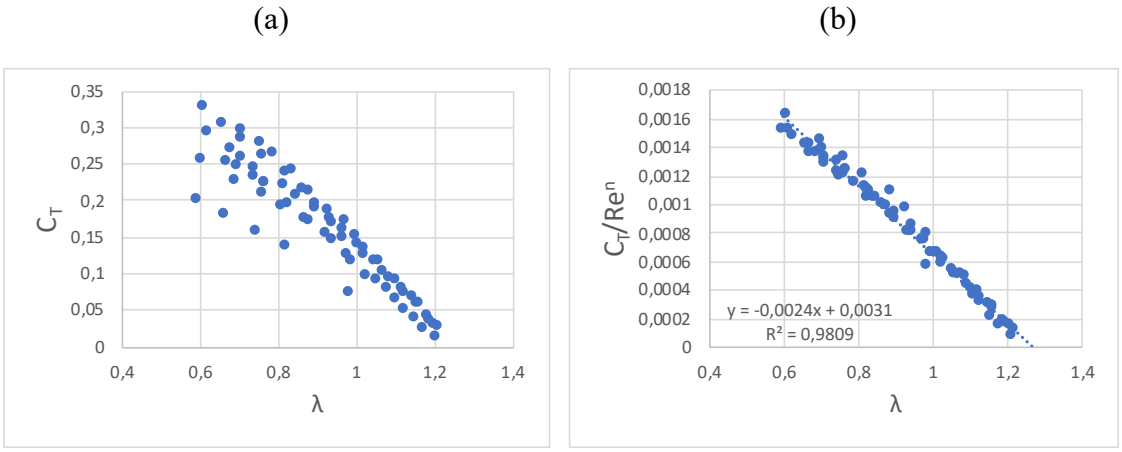

Figure 21. Torque coefficients (a) and linear correlation (b) of a helical SWT with 90-degree twist, an aspect ratio of 0.88 and no overlap ratio. The optimal exponent used with the correlation was 0.446. Tests are conducted with Reynolds numbers 57702, 86554, 115405, 144256, 173107 and 201958. Data is collected from an experimental study (Kamoji et al., 2009b, p. 526, fig. 8).

The study also included a performance comparison of two helical SWT variants and conventional SWT. The aspect ratios of the helical variants were 0.88 and 0.96 and the overlap ratios were 0 and 0.10 respectively. The aspect ratio of a conventional SWT was 0.10 and the overlap ratio was 0.15.

5.1.5 **Modified SWT variants by Mercado-Colmenero et al.**

Colmenero et al. studied the performance of a modified SWT experimentally. Tests also included a conventional SWT with the same aspect ratio for comparison. Experimental setup used an open jet wind tunnel to measure power coefficients, torque coefficients and

mechanical power of the rotor. Tests were conducted with Reynolds number values between 34300 and 141900. Measurements take place roughly between TSR values of 0.0 and 0.7. Basic dimensions for the modified rotor variants is visible in table 6. (Mercado-Colmenero et al., 2018, p. 210)

Table 6. Basic dimension ranges with Reynolds numbers and tip–to–speed ratios used in this analysis for standard SWT and prototype rotor (Mercado-Colmenero et al., 2018).

Rotor diameter	d	[m]	Variable
Rotor height	h	[m]	0.320
Rotor aspect ratio	h/d	[-]	1.618
Rotor overlap ratio	o	[-]	0.326–0.343
Number of blades	n_b	[-]	2
Number of stages	n_s	[-]	1
Tip–to–speed ratio	λ	[-]	0.07–0.66
Reynolds number	Re	[-]	34400–142000

Figure 22 shows the performance of a SWT with 45-degree twist angle. Torque coefficients measured in the experimental study are shown in figure 22(a). Figure 22(b) shows the correlation formed from the experimental data with a correlation exponent of 1.192. The value of the exponent is significantly different from the other studies in which it was usually close to 0.3. Additionally, the average exponent for all of the analysed studies is 0.293 for a polynomial correlation. The coefficient of determination for the polynomial curve is 0.963, which is noticeably higher than the coefficient of determination of 0.932 achieved with the linear correlation. Due to the high correlation exponent, correlation values against TSR are unusually low. The formed polynomial correlation curve is shown in following equation.

$$\frac{C_T}{Re^{1.192}} = -6.622 \cdot 10^{-7} \cdot \lambda^2 - 9.402 \cdot 10^{-7} \cdot \lambda + 3.396 \cdot 10^{-7} \qquad (16)$$

(a) (b)

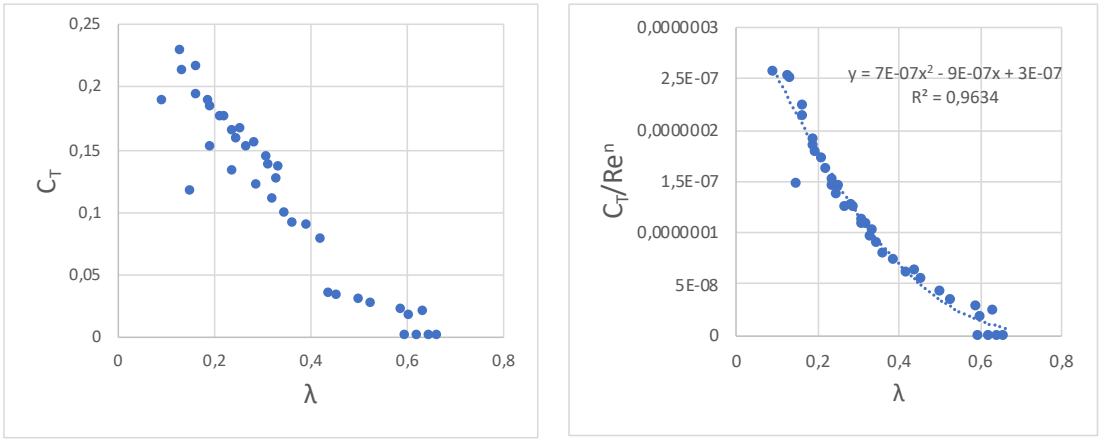

Figure 22. Torque coefficients (a) and a linear correlation curve of a SWT with a twist angle of 45 degrees. The correlation curve was achieved with a correlation exponent of 1.192, which resulted in a coefficient of determination of 0.963. (Mercado-Colmenero et al., 2018, p. 222, fig. 13)

In addition to the variant with the 45-degree twist angle, the study also had two modified SWT variants with different twist angles of 0 degrees and 22.5 degrees and one conventional SWT. The optimal correlation curves were calculated which resulted in unclear results. The data from the conventional SWT had too little amount of data points to get a clear picture. The two other variants had some possibility for linear or polynomial correlations, but the data points were somewhat scattered even with the optimal correlation exponent. The optimal correlation exponents were also higher than average ones. varied between 0.590 and 0.821 for the linear correlations and 0.576 and 0.835 for the polynomial correlations. The coefficients of determination were relatively low between 0.869 and 0.93 for the turbines excluding the variant with a twist angle of 45°.

5.1.6 **Helical modified SWT variants by Damak et al.**

Damak et al. studied the performance of a helical SWT through wind tunnel experiments. More specifically, the rotor used in the experiments is a Bach-type SWT. The combination of the Bach rotor with helical rotor is meant to reduce the areas of negative torque on Bach rotors. In addition, the power coefficient of a helical rotor could be increased due to higher power coefficient of Bach rotors. The experimental setup includes open wind tunnel and a helical Bach rotor made of resin and glass fibre. The experiment included power coefficients, torque coefficients and static torque coefficients from which torque coefficients were collected. Table 7 shows some basic dimensions for the helical rotor and helical Bach rotor. (Damak et al., 2018)

Table 7. Basic dimensions with Reynolds numbers and tip–to–speed ratios used in this analysis for the helical Bach rotor and helical rotor (Damak et al., 2018).

Rotor diameter	d	[m]	0.230
Rotor height	h	[m]	0.162
Rotor aspect ratio	h/d	[-]	0.7
Rotor overlap ratio	o	[-]	0
Number of blades	n_b	[-]	2
Number of stages	n_s	[-]	1
Tip–to–speed ratio	λ	[-]	0.5–1.3
Reynolds number	Re	[-]	73700–131600

Figure 23 shows the performance of a helical Bach rotor. To achieve more uniform results with other studies, data points were only analysed when TSR was over 0.5. Torque coefficients for the helical Bach rotor are shown in the figure 23(a) while the formed correlation curve is shown in the figure 23(b). The optimal correlation exponent was found to be 0.247 for the polynomial curve, which resulted in a coefficient of determination of 0.988.

Data from the helical Bach rotor forms a polynomial correlation shown in the following equation.

$$\frac{C_T}{Re^{0.247}} = -0.0219 \cdot \lambda^2 + 0.0129 \cdot \lambda + 0.0135 \quad (17)$$

(a) (b)

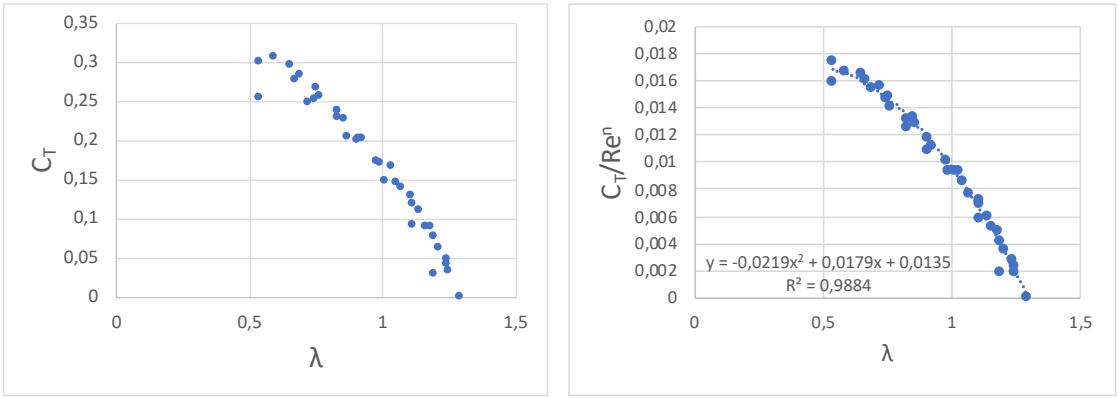

Figure 23. Torque coefficients for the helical Bach rotor (a) and correlation curve for the same rotor (b). The figure includes measured torque coefficients (a) and polynomial correlation (b). The correlation was achieved with a correlation exponent of 0.247. Data is collected from an experimental study (Damak et al., 2018, pp. 86–87, fig. 9-10).

Figure 24 shows the performance of a helical rotor. Torque coefficients for the helical rotor are visible in figure 24(c) and correlation curve for the same rotor is visible in the figure 24(d). The correlation curve shown in the figure 24(d) is polynomial. In this case, the linear correlation also resulted in relatively high coefficient of determination especially when TSR is over 0.6. The formed correlation is shown in the following equation.

$$\frac{C_T}{Re^{0.209}} = -0.0241 \cdot \lambda^2 + 0.0066 \cdot \lambda + 0.029 \quad (18)$$

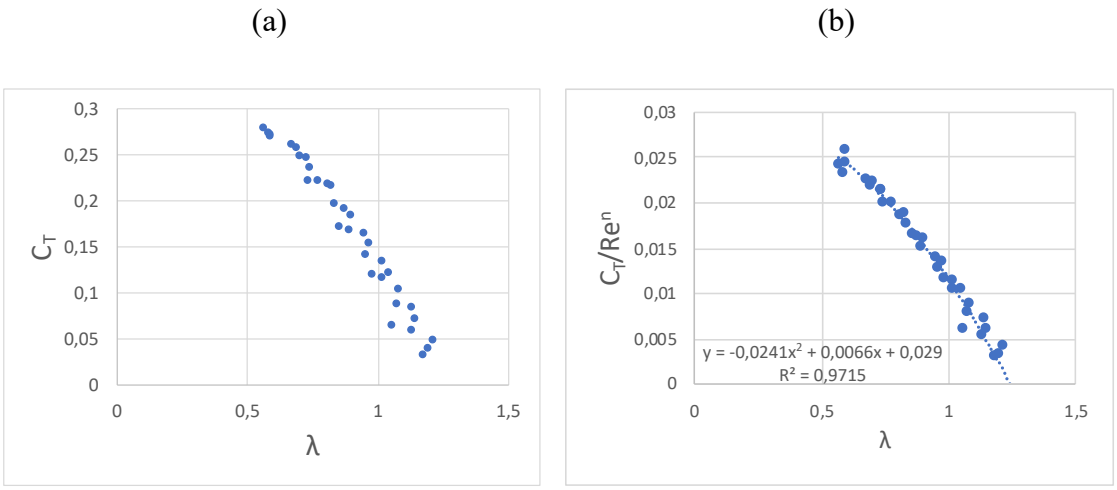

Figure 24. Torque coefficients for the helical rotor (a) and polynomial correlation curve for the same rotor (b). The optimal correlation curve was achieved with a correlation exponent of 0.209. Data is collected from an experimental study (Damak et al., 2018, pp. 86–87, fig. 9-10).

5.1.7 Conventional SWT variants by Blackwell et al.

Blackwell et al. studied the performance of a SWT with two and three blades between two end plates all made of aluminium alloy. In addition to the blade number, the experiment included multiple different design parameters, and their effect on the performance. Rotors were positioned at the centre of the wind tunnel to achieve optimal measurement results. Basic dimension ranges for the rotors used in the study are visible in the table 8. (Blackwell et al., 1977, p. 15)

Rotor variants with two buckets used blades with 180-degree arc angles and an arc radius of 0.25 meters. The study uses dimensionless gap width, which means overlap ratio, as variable parameter in experiments. Three-bladed variants mostly used blades with an arc angle of 150 degrees and arc radius of 0.25 meters. Gap distance is a parameter used in

the study, that indicates the length between inner edge of the blade and centre of the rotor axis. (Blackwell et al., 1977, p. 20)

Table 8. Basic dimensions with Reynolds numbers and tip–to–speed ratios used in this analysis for the helical Bach rotor and the helical rotor (Blackwell et al., 1977).

Rotor diameter	d	[m]	0.8888–1.0024
Rotor height	h	[m]	1.0–1.5
Rotor aspect ratio	h/d	[-]	1.013–1.688
Rotor overlap ratio	o	[-]	0.0–0.2
Number of blades	n_b	[-]	2–3
Number of stages	n_s	[-]	1
Tip–to–speed ratio	λ	[-]	0.5–1.4
Reynolds number	Re	[-]	432000–867000

A total of 13 figures from the study were analysed. Different figures featured different design configurations with varying overlap ratio, blade arc angle, rotor aspect ratio and number of blades. All of the tests were measured with two Reynolds numbers, either from 432000 to 864000 or from 433000 to 867000. The small amount of Reynolds numbers less reliable to find the optimal correlations and exponents.

The optimal exponents for both the linear and polynomial correlations were on the lower side. The highest exponent for any of the figures from the study was 0.107 for the polynomial correlation and 0.0927 for the linear correlation. Some of the figures had an optimal exponent of 0, which means no correlation that could increase the accuracy of the curve existed. Even though correlation may not be reliable, the shape of the curve can still be examined. Generally, all of the examined figures achieved high coefficients of

determination. All of the coefficients were over 0.98. This is because the torque coefficients from the study do not change much between the two Reynolds numbers.

The performance of a SWT with two blades, an overlap ratio of 0.2 and a height of 1.0 meter is shown in figure 25. The torque coefficients measured in the experimental study are visible in figure 25(a) and the optimal linear correlation for the same rotor is in figure 25(b). As can be seen from the torque coefficients, the data points are not very scattered. Additionally, the correlation curve clearly seems to be linear. The optimal exponent for the linear correlation was found to be 0.0927, which gave a coefficient of determination of 0.997. A coefficient of determination for the polynomial correlation was almost the same, which confirms the validity of the linear correlation. A following equation was achieved with the exponent of the linear correlation.

$$\frac{C_T}{Re^{0.0927}} = -0.091 \cdot \lambda + 0.1562 \tag{19}$$

(a) (b)

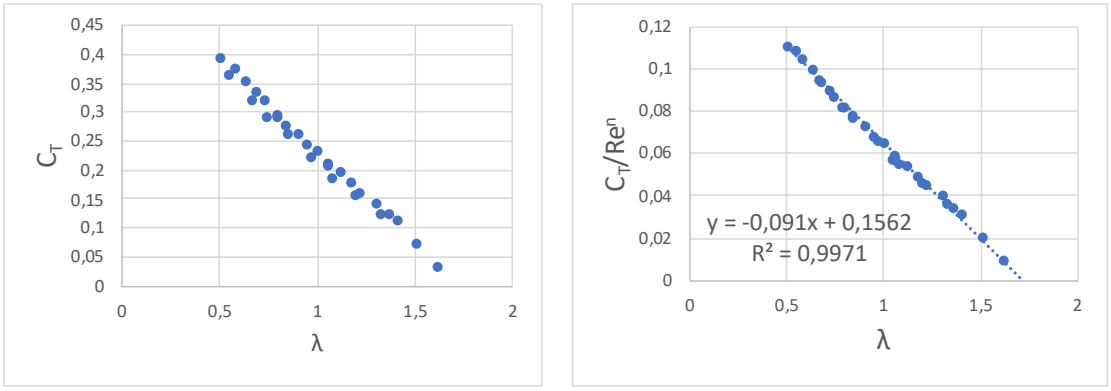

Figure 25. Torque coefficients (a) and linear correlation (b) from a SWT with two blades, an overlap ratio of 0.2 and a height of 1 meter. Linear correlation equation was achieved with a correlation exponent of 0.0927 which resulted in coefficient of determination of 0.997. (Blackwell et al., 1977, p. 49, fig. 17)

Other 12 figures are not presented in this section due to high similarities with the previous figure. All of the other figures clearly resulted in linear correlation equations. This once

again suggests that changing the overlap ratio, the number of blades or the rotor aspect ratio does not notably affect the shape of the correlation curve.

5.2 Summary of the measurement results

Due to the large amount of examined data and very similar results between some of the figures, not all of the figures were included in previous sections. Summarized results from all studied turbine models can be found in the appendix I. In this section, summaries for individual studies are included rather than individual experiments.

The experimental study by Grönman et al. used a vaned SWT with three blades. The formed correlation was clearly second order. Experimental data mostly fit the correlation with an error of 5 %. Torque coefficients were measured with TSR values being between 0.4 and 1.0. Reynolds numbers varied between 886300 and 221600, which were mostly much higher than those of other studies examined here.

Three studies by Kamoji et al. were examined all with different SWT variants. The experimental study by Kamoji et al. with single stage, two stage and three stage SWT variants resulted in somewhat clear non-linear curves for all turbine variants. If only the correlation values after TSR of 0.6 are taken into account, correlation curves seem to be very clearly linear. Reynolds numbers were between 77600 and 168500 for figures examined here. Another study by Kamoji et al. with modified single stage SWT resulted in similar linear values when fit into torque coefficient initial condition. Most of the measurements were done under two Reynolds numbers of 120000 and 150000. The study also included two figures with torque coefficients and correlation curve values where Reynolds numbers were between 77600 and 150000. Third study by Kamoji et al. had helical SWT. Correlation curve values were clearly linear on all of the studied turbine variants when TSR was higher than 0.5. TSR values lower than 0.5 clearly started to level off or turn downwards. Lower TSR values were not included in the analysis since those data points were more scattered and there was less available data overall.

The results from the experimental study by Colmenero et al. clearly formed a second order correlation especially in figure 22(c). Values from the other figures did not show as clear signs of a correlation or direction of such correlation. It is notable that tests in this experiment were conducted with much lower TSR values between 0.05 and 0.7. Correlation curves for this study were bending upwards. Reynolds numbers varied between 71400 and 142000 in examined figures.

Blackwell et al. studied the performance of SWT mostly on two different Reynolds numbers in the range of 432000–864000. While two Reynolds numbers does not give much confidence to conclusions, all results were clearly formed linearly when TSR values were over 0.5.

Data that is fit into the initial condition of the performance correlation seems to have the same form as the curve for the torque coefficient only. To find out what affects the form of the torque coefficient curve, more data about torque coefficient is needed.

Damak et al. studied the performance of a helical SWT and a Helical Bach rotor. The studied torque coefficient data formed a somewhat gently curved polynomial correlation curve. The figures 23 and 24 presented previously showed only polynomial correlation equations. Linear equations also formed relatively correlations with relatively high coefficients of determination as shown in the appendix I. (Damak et al., 2018)

Overwhelming majority of the correlation curves were very close to linear when TSR was over 0.5. Only three clear polynomial curves were found. Those curves were from studies by Colmenero et al. and Grönman et al. All of the curves by those studies were either polynomial or not clear for the Reynolds number range that was investigated.

5.3 Factors affecting measurement results

Both aforementioned studies by Grönman et al. and Mercado-Colmenero et al. achieved similar curve shape with a possibility for a high accuracy second order correlation. Neither of the studies used conventional Savonius rotors. The shape of the curve indicates

relatively higher performance on lower TSR values. The study by Grönman et al. used a three-bladed SWT with stator vanes to concentrate the flow. The relatively higher performance on low TSR could be explained with vanes accelerating the flow relatively more on the low TSR as suggested in the original study (Grönman et al., 2019, p. 867). The rotors used in the study by Mercado-Colmenero et al. were unusual modified Savonius rotors with vertically curved blades. The most accurate second-order polynomial graph in the study was the one with the highest twist angle.

The figures related to multiple staged SWT variants by Kamoji et al. featured a more or less accurate linear stack of data. One exception was that the linear form started to turn down, when TSR was lower than 0.6 (Kamoji et al., 2008). Similar linear results were achieved with the two other studies by Kamoji et al. with modified rotor and helical rotor, which would indicate, that adding twist to the blades does not alone explain the shape of the correlation on the study by Mercado-Colmenero et al. The range of the TSR is also a lot lower than those of the other studies, which could explain the higher exponent. (Mercado-Colmenero et al., 2018)

The data from the study by Damak et al. featured second-order polynomial forms at least on the figure 24(a). Shapes of the curves on the figure 24 resemble some of the graphs on the study by Kamoji et al. on multiple staged turbines (Kamoji et al., 2008). Torque coefficients form most of the other studies start to deteriorate when TSR is under 0.6. Similar behaviour is seen in the study by Damak et al. and it could explain the slightly curved equations (Damak et al., 2018).

Data from Blackwell et al. formed linear shapes on almost all of the figures and over all of the TSR values. The study used only conventional straight-bladed SWT models. The largest optimal correlation exponent was found to be 0.107. In three of the figures, the correlation only made the data more scattered, which means that the optimal correlation exponent was found to be 0. Since Blackwell et al. studied the performance of conventional SWT variants and all of the correlations featured unusually low correlation exponents the new correlation may not be suitable for such high Reynolds numbers. On the

other hand, the experiments in the study were only conducted with two Reynolds numbers, which already makes any conclusions somewhat inaccurate. (Blackwell et al., 1977).

5.3.1 Correlation exponents

Exponent of the correlation affects how the correlation moves the torque coefficient data from different Reynolds numbers relative to each other. The exponent does not seem to affect the shape of the correlation much other than by changing the positions of the data points closer to each other. As suggested by other studies, the range of Reynolds of numbers does not seem to dictate the shape of the correlation either. The correlation curve mostly follows the form of the torque coefficient data. To get some idea how the exponent should be chosen for each correlation curve, the effect of some parameters is examined in this section.

Common design parameters of the SWT seem to affect the optimal value of the correlation exponent. In the study by Kamoji et al. on single-, two- and three-stage SWT variants, the correlation exponent varied from 0.168 to 0.735. A higher aspect ratio seems to lead a higher correlation exponent. Aspect ratio increases the rotational speed and reduces the torque transmitted to the shaft, which could explain more scattered data points from SWTs with higher aspect ratios. On the other hand, Reynolds numbers are also a lot lower on the variants with higher aspect ratios due to the lower starting torque. The exponents used in correlations formed from the data by Kamoji et al. is shown in table 9.

Table 9. Exponents for linear correlations formed from the data from the experimental study by by Kamoji et al. (Kamoji et al., 2008)

Rotor aspect ratio	Stage aspect ratio	Optimal linear correlation exponent
1	1	0.206
1	0.5	0.168
2	1	0.380
1	0.33	0.265

3	1	0.735

Many of the examined experiments studied the effect of the overlap ratio on the performance of multiple SWTs. While the overlap ratio did not notably affect the shape of a correlation curve, its effect on the correlation exponent is examined in this section. Kamoji et al. studied the performance of a single stage SWT with an aspect ratio of 0.77 and three different overlap ratios of 0.0, 0.10 and 0.16. (Kamoji et al., 2008, p. 1067, fig. 5-6). The optimal correlation exponents were found to be 0.180, 0.508 and 0.0. Kamoji et al. also studied the effect of overlap ratio for a helical SWT (Kamoji et al., 2009b, pp. 524–525, fig. 5-6). Three helical variants with no central shaft are examined with overlap ratios of 0.0, 0.10 and 0.16 and aspect ratios of 0.88, 0.96 and 1.0. The optimal correlation exponents were 0.402, 0.617 and 0.474 respectively for the linear correlation. Blackwell et al. also studied the effect of the overlap ratio for multiple two- and three-bladed SWT variants (Blackwell et al., 1977). Since all of the optimal correlation exponents for the study are either 0 or close to 0, no conclusion can be drawn from here. The overlap ratio seems to either have a small impact on the exponent or other parameters affect the exponent more. The experiments studied in this section were conducted with only two different Reynolds numbers, which makes the optimal correlation exponent inaccurate.

Blade arc angle had varied between 124 and 180 degrees in studied experiments for two-bladed SWTs. Only one study by Kamoji et al. studied the effect of blade arc angle on the performance using four SWT variants (Kamoji et al., 2009a, p. 1069, fig. 9-10). The study used blade arc angles of 110, 124, 135 and 150 degrees, and the optimal linear correlation curves were achieved with exponents of 0.156, 0.080, 0.744 and 0.332 respectively. There is a large variance in the exponents and no clear indicator whether the arc angle affects those exponents.

5.3.2 Shape of the correlation curve

The formation in which the data points of torque coefficients settle in is clearly different between some of the studies and is related to large design differences. No change in the curve shape was observed when the effect of the typical design parameters was examined. Typical examined parameters include the effect of the overlap ratio, the aspect ratio, the blade shape factor, the number of blades or the blade arc angle. Studies that had clear linear correlations did not have clear polynomial correlations on any of the variants. In addition, the studies that resulted in at least one clear polynomial correlation, did not have any clearly linear correlations.

Polynomial correlations were observed with studies from Damak et al., Colmenero et al. and Grönman et al. Studies from Colmenero et al. and Grönman et al. had upwards bending correlation curve, while study from Damak et al. had a downwards bending one. The curve from the study by Damak et al. was clearly second order when it was examined on the whole TSR range. After the TSR range was limited to higher than 0.5, the coefficient of determination of a linear curve became higher. The same thing was observed with some of the figures from all of the studies by Kamoji et al. when enough Data was available. The relative performance starts to deteriorate at low TSR. The curve of those figures became more like the those of the study by Damak et al.

Due to the low amount of data available from turbines similar to the studies that resulted in polynomial correlation, it’s not possible to draw accurate conclusions on reasons behind the polynomial shape. Since almost all of the correlation curves were close to linear at least when TSR is over 0.5, the correlation equation can be applied to the majority of the SWT designs. On the other hand, the optimal correlation exponent range was rather large, which makes the performance estimates somewhat inaccurate.

6 CONCLUSIONS

Savonius wind turbine is a wind turbine with clear advantages and disadvantages. Still, the low performance of the turbine is a limiting factor for a large-scale energy production. Most of the worlds wind energy may continue to be generated by horizontal axis wind turbines. This does not rule out the clear advantages the Savonius wind turbine has especially for rural and urban areas where low noise, self-starting capabilities and compact size may matter more than high efficiency.

The performance of the Savonius wind turbine can be optimized with numerous different design parameters. Blades of the Savonius wind turbine have concave and convex side. In order to increase the power output and efficiency of the rotor, the flow of air into the concave side of the blade needs to be maximized. The blade that is moving in the same direction as the wind, is called advancing blade while the other blade is called returning blade.

Some of the parameters such as inclusion and optimal size of the end plates can increase the performance notably. Performance improvement can also be achieved with stator vanes around the rotor. Using additional structures around the rotor leads to increased weight and size. Some parameters such as blade twist and blade number can be used to even out the static torque distribution on the shaft. Using higher aspect ratio can increase the rotational speed while reducing the torque. The rest of the investigated parameters did not have such a clear effect on the performance. The Reynolds number on the other hand has been studied thoroughly and the consensus is that increasing the Reynolds number does increase the power coefficient of a Savonius wind turbine. In addition, using stator vanes or vertically curved blades can increase the performance when turbine is in an environment with low wind speeds.

In this thesis, the form of the new correlation developed for the Savonius wind turbine performance was examined. This correlation has been suggested by several studies in the past with slightly different results. In order to reliably study the behaviour of the correlation, multiple correlation curves were made from the data from multiple other studies. A

total of 52 figures were examined. The figures were from seven different studies conducted between 1977 and 2019. Results from multiple studies were not always consistent.

Applying the correlation did make the data points from the figures at least a little bit less scattered on almost all of the cases. Previously developed correlations in studies that were examined were either linear or polynomial equations. The overwhelming majority of the studied torque coefficient data formed a linear curve when TSR was over 0.5. When TSR was under 0.5, the relative performance started to deteriorate. The amount of data on low TSR range was sometimes too scarce to be included in the correlation equation. For this reason, studied data points were limited to tip–to–speed ratios of over 0.5 for most of the studies. It was concluded that most of the typical design parameters did not notably affect the shape of the correlation curve. Only one of the examined studies included stator vanes around the rotor. The same study also was one of the few that had formed a polynomial correlation curve. The only other case where upwards bending polynomial curve was observed was with a modified SWT where the blades had been curved vertically. No other sufficiently comprehensive studies with similar dimensions were found.

The optimal exponent of the correlation equation was sought for all of the 52 examined figures. The optimal correlation exponents were between 0 and 0.8 for polynomial correlation. and between 0 and 1.192 for linear correlations. Mean exponents for all of the examined studies was 0.293 for polynomial correlations and 0.272 for linear correlations. Since the data from most of the studies was close to linear when tip–to–speed ratio was over 0.5, a linear correlation applied into this range could be applied into majority of different Savonius wind turbine designs available. In this case, finding the optimal exponent for the correlation is another task that requires attention. It was concluded, that the optimal exponent was clearly higher with higher turbine aspect ratios. Other investigated parameters did not have a clear effect on the exponent. To find other parameters that affect the optimal correlation exponent, the effect of other typical design parameters should be investigated with a wider range of Reynolds numbers in otherwise similar turbine configurations.

REFERENCES

Abraham, J., Plourde, B., Mowry, G., Minkowycz, W., Sparrow, E., 2012. Summary of Savonius wind turbine development and future applications for small-scale power generation. Journal of Renewable and Sustainable Energy 4. https://doi.org/10.1063/1.4747822

Akwa, J.V., Vielmo, H.A., Petry, A.P., 2012. A review on the performance of Savonius wind turbines. Renewable and Sustainable Energy Reviews 16, 3054–3064. https://doi.org/10.1016/j.rser.2012.02.056

Altan, B.D., Atılgan, M., 2012. A study on increasing the performance of Savonius wind rotors. J Mech Sci Technol 26, 1493–1499. https://doi.org/10.1007/s12206-012-0313-y

Altan, B.D., Atılgan, M., 2010. The use of a curtain design to increase the performance level of a Savonius wind rotors. Renewable Energy 35, 821–829. https://doi.org/10.1016/j.renene.2009.08.025

Blackwell, B.F., Sheldahl, R.E., Feltz, L.V., 1977. Wind tunnel performance data for two- and three-bucket Savonius rotors (No. SAND-76-0131). Sandia Labs., Albuquerque, NM (USA).

Damak, A., Driss, Z., Abid, M.S., 2018. Optimization of the helical Savonius rotor through wind tunnel experiments. Journal of Wind Engineering and Industrial Aerodynamics 174, 80–93. https://doi.org/10.1016/j.jweia.2017.12.022

El-Askary, W.A., Saad, A.S., AbdelSalam, A.M., Sakr, I.M., 2018. Investigating the performance of a twisted modified Savonius rotor. Journal of Wind Engineering and Industrial Aerodynamics 182, 344–355. https://doi.org/10.1016/j.jweia.2018.10.009

Grönman, A., Tiainen, J., Jaatinen-Värri, A., 2019. Experimental and analytical analysis of vaned savonius turbine performance under different operating conditions.

Hau, E., 2013. Basic Concepts of Wind Energy Converters, in: Hau, E. (Ed.), Wind Turbines: Fundamentals, Technologies, Application, Economics. Springer, Berlin, Heidelberg, pp. 65–78. https://doi.org/10.1007/978-3-642-27151-9_3

IEA, 2019. Renewables 2019.

IRENA, 2019. Statistics Time Series [WWW Document]. /Statistics/View-Data-by-Topic/Capacity-and-Generation/Statistics-Time-Series. URL https://www.irena.org/Statistics/View-Data-by-Topic/Capacity-and-Generation/Statistics-Time-Series (accessed 2.4.20).

James, P.A.B., Bahaj, A.S., 2017. Chapter 19 - Small-Scale Wind Turbines, in: Letcher, T.M. (Ed.), Wind Energy Engineering. Academic Press, pp. 389–418. https://doi.org/10.1016/B978-0-12-809451-8.00019-9

Jeon, K.S., Jeong, J.I., Pan, J.-K., Ryu, K.-W., 2015. Effects of end plates with various shapes and sizes on helical Savonius wind turbines. Renewable Energy, Selected Papers on Renewable Energy: AFORE 2013 79, 167–176. https://doi.org/10.1016/j.renene.2014.11.035

Johari, M.K., Jalil, M.A.A., Shariff, M.F.M., 2018. Comparison of horizontal axis wind turbine (HAWT) and vertical axis wind turbine (VAWT). https://doi.org/10.14419/ijet.v7i4.13.21333

Kalmikov, A., 2017. Chapter 2 - Wind Power Fundamentals, in: Letcher, T.M. (Ed.), Wind Energy Engineering. Academic Press, pp. 17–24. https://doi.org/10.1016/B978-0-12-809451-8.00002-3

Kamoji, M.A., Kedare, S.B., Prabhu, S.V., 2009a. Experimental investigations on single stage modified Savonius rotor. Applied Energy 86, 1064–1073. https://doi.org/10.1016/j.apenergy.2008.09.019

Kamoji, M.A., Kedare, S.B., Prabhu, S.V., 2009b. Performance tests on helical Savonius rotors. Renewable Energy 34, 521–529. https://doi.org/10.1016/j.renene.2008.06.002

Kamoji, M.A., Kedare, S.B., Prabhu, S.V., 2008. Experimental investigations on single stage, two stage and three stage conventional Savonius rotor. International Journal of Energy Research 32, 877–895. https://doi.org/10.1002/er.1399

Kim, S., Cheong, C., 2015. Development of low-noise drag-type vertical wind turbines. Renewable Energy, Selected Papers on Renewable Energy: AFORE 2013 79, 199–208. https://doi.org/10.1016/j.renene.2014.09.047

Lee, J.-H., Lee, Y.-T., Lim, H.-C., 2016. Effect of twist angle on the performance of Savonius wind turbine. Renewable Energy 89, 231–244. https://doi.org/10.1016/j.renene.2015.12.012

Letcher, T. M, 2017. Wind energy engineering: a handbook for onshore and offshore wind turbines.

Letcher, Trevor M., 2017. Chapter 1 - Why Wind Energy?, in: Letcher, T.M. (Ed.), Wind Energy Engineering. Academic Press, pp. 3–14. https://doi.org/10.1016/B978-0-12-809451-8.00001-1

Lydia, M., Kumar, S.S., Selvakumar, A.I., Prem Kumar, G.E., 2014. A comprehensive review on wind turbine power curve modeling techniques. Renewable and Sustainable Energy Reviews 30, 452–460. https://doi.org/10.1016/j.rser.2013.10.030

Mao, Z., Tian, W., 2015. Effect of the blade arc angle on the performance of a Savonius wind turbine. Advances in Mechanical Engineering; New York 7, 1–10. http://dx.doi.org.ezproxy.cc.lut.fi/10.1177/1687814015584247

Mercado-Colmenero, J.M., Rubio-Paramio, M.A., Guerrero-Villar, F., Martin-Doñate, C., 2018. A numerical and experimental study of a new Savonius wind rotor adaptation based on product design requirements. Energy Conversion and Management 158, 210–234. https://doi.org/10.1016/j.enconman.2017.12.058

Molina, M., Mercado, P., 2011. Modelling and Control Design of Pitch-Controlled Variable Speed Wind Turbines. https://doi.org/10.5772/15880

Montelpare, S., D'Alessandro, V., Zoppi, A., Ricci, R., 2018. Experimental study on a modified Savonius wind rotor for street lighting systems. Analysis of external appendages and elements. Energy 144, 146–158. https://doi.org/10.1016/j.energy.2017.12.017

Morshed, K.N., Rahman, M., Molina, G., Ahmed, M., 2013. Wind tunnel testing and numerical simulation on aerodynamic performance of a three-bladed Savonius wind turbine. Int J Energy Environ Eng 4, 18. https://doi.org/10.1186/2251-6832-4-18

Pan, H., Li, H., Zhang, T., Laghari, A.A., Zhang, Z., Yuan, Y., Qian, B., 2019. A portable renewable wind energy harvesting system integrated S-rotor and H-rotor for self-powered applications in high-speed railway tunnels. Energy Conversion and Management 196, 56–68. https://doi.org/10.1016/j.enconman.2019.05.115

Poudineh, R., Brown, C., Foley, B., 2017. Background: Role of the Offshore Wind Industry, in: Poudineh, R., Brown, C., Foley, B. (Eds.), Economics of Offshore Wind Power: Challenges and Policy Considerations. Springer International Publishing, Cham, pp. 1–14. https://doi.org/10.1007/978-3-319-66420-0_1

Riegler, H., 2003. HAWT versus VAWT: Small VAWTs find a clear niche. Refocus 4, 44–46. https://doi.org/10.1016/S1471-0846(03)00433-5

Roy, S., Saha, U.K., 2013. Review on the numerical investigations into the design and development of Savonius wind rotors. Renewable and Sustainable Energy Reviews 24, 73–83. https://doi.org/10.1016/j.rser.2013.03.060

Rus, T., Rus, L.F., Ilutiu-Varvara, D.A., Mare, R., Abrudan, A., Domnita, F., 2018. Experimental Investigation on the Influence of Overlap Ratio on Savonius Turbines Performance. International Journal of Renewable Energy Research (IJRER) 8, 1791–1799.

Santhakumar, S., Palanivel, I., Venkatasubramanian, K., 2018. An experimental study on the rotational behaviour of a Savonius wind turbine for two-lane highway applications. J Braz. Soc. Mech. Sci. Eng. 40, 232. https://doi.org/10.1007/s40430-018-1158-9

Savonius, S.J., 1931. The S-Rotor and Its Applications. Mechanical Engineering 53, 333–338.

Tjiu, W., Marnoto, T., Mat, S., Ruslan, M.H., Sopian, K., 2015. Darrieus vertical axis wind turbine for power generation II: Challenges in HAWT and the opportunity of multi-megawatt Darrieus VAWT development. Renewable Energy 75, 560–571. https://doi.org/10.1016/j.renene.2014.10.039

Tummala, A., Velamati, R.K., Sinha, D.K., Indraja, V., Krishna, V.H., 2016. A review on small scale wind turbines. Renewable and Sustainable Energy Reviews 56, 1351–1371. https://doi.org/10.1016/j.rser.2015.12.027

U.S. Department of Energy, 1977. HD.11C.030.

U.S. Department of Energy, n.d. The Inside of a Wind Turbine [WWW Document]. Energy.gov. URL https://www.energy.gov/eere/wind/inside-wind-turbine (accessed 5.19.20).

Wenehenubun, F., Saputra, A., Sutanto, H., 2015. An Experimental Study on the Performance of Savonius Wind Turbines Related With The Number Of Blades. Energy Procedia, 2nd International Conference on Sustainable Energy Engineering and Application (ICSEEA) 2014 Sustainable Energy for Green Mobility 68, 297–304. https://doi.org/10.1016/j.egypro.2015.03.259

Whittlesey, R., 2017. Chapter 10 - Vertical Axis Wind Turbines: Farm and Turbine Design, in: Letcher, T.M. (Ed.), Wind Energy Engineering. Academic Press, pp. 185–202. https://doi.org/10.1016/B978-0-12-809451-8.00010-2

Zemamou, M., Aggour, M., Toumi, A., 2017. Review of savonius wind turbine design and performance. Energy Procedia, Power and Energy Systems Engineering 141, 383–388. https://doi.org/10.1016/j.egypro.2017.11.047

Zhou, T., Rempfer, D., 2013. Numerical study of detailed flow field and performance of Savonius wind turbines. Renewable Energy 51, 373–381. https://doi.org/10.1016/j.renene.2012.09.046

APPENDIX I. SUMMARIZED RESULTS FROM EXPERIMENTAL DATA

	Type	Figure in the study	No. of blades	No. of stages	n_{Re}	Re (min)	Re (max)	Aspect ratio	Twist	Arc angle	Overlap ratio	n poly	n linear	R^2 poly	R^2 linear	Correlation shape
Blackwell et al. 1977	Conventional	Fig. 15	2	1	2	432000	864000	1	0	180	0,1	0,025	0,023	0,994	0,994	Linear
	Conventional	Fig. 16	2	1	2	432000	864000	1	0	180	0,15	0,020	0,021	0,997	0,996	Linear
	Conventional	Fig. 17	2	1	2	432000	864000	1	0	180	0,2	0,093	0,093	0,997	0,997	Linear
	Conventional	Fig. 19	2	1	2	433000	867000	1,5	0	180	0,1	0,000	0,000	0,998	0,998	No correlation
	Conventional	Fig. 20	2	1	2	433000	867000	1,5	0	180	0,15	0,000	0,000	0,998	0,998	No correlation
	Conventional	Fig. 29	3	1	2	432000	864000	1	0	180	0	0,039	0,040	0,998	0,997	Linear
	Conventional	Fig. 30	3	1	2	432000	864000	1	0	150	0,1	0,018	0,015	0,995	0,994	Linear
	Conventional	Fig. 31	3	1	2	432000	864000	1	0	150	0,15	0,076	0,076	0,997	0,997	Linear
	Conventional	Fig. 32	3	1	2	432000	864000	1	0	150	0,2	0,024	0,001	0,990	0,988	Linear
	Conventional	Fig. 33	3	1	2	433000	867000	1,5	0	150	0	0,043	0,041	0,997	0,997	Linear
	Conventional	Fig. 34	3	1	2	432000	864000	1,5	0	150	0,1	0,000	0,000	0,988	0,988	No correlation
	Conventional	Fig. 35	3	1	2	433000	867000	1,5	0	150	0,2	0,059	0,064	0,996	0,995	Linear
	Conventional	Fig. 36	3	1	2	433000	867000	1,5	0	150	0,2	0,107	0,034	0,997	0,992	Linear
Damak et al. 2018	Helical Bach	Fig. 9	2	1	4	73700	131600	0,7	90	124	0	0,247	0,314	0,988	0,954	Polynomial
	Helical	Fig. 10	2	1	4	73700	131600	0,7	90	180	0	0,209	0,331	0,971	0,957	Polynomial
Grönman et al. 2019	Vaned	Fig. 3	3	1	7	221600	886300	0,52	0	120	0,1015	0,273	0,190	0,994	0,946	Polynomial
Kamoji et al. 2008 Conventional single, two and three stage	Conventional	Fig. 5	2	1	4	77600	155000	1	0	180	0,15	0,206	0,208	0,983	0,982	Linear
	Conventional	Fig. 7	2	2	4	84500	168500	1	0	180	0,15	0,168	0,147	0,992	0,978	Linear
	Conventional	Fig. 8	2	2	4	48900	97800	2	0	180	0,15	0,380	0,381	0,949	0,947	Linear
	Conventional	Fig. 10	2	3	4	84000	168000	1	0	180	0,15	0,265	0,255	0,985	0,982	Linear
	Conventional	Fig. 11	2	3	4	36000	72000	3	0	180	0,15	0,735	0,708	0,848	0,845	Linear
Kamoji et al. 2009a Experimental investigations on single stage modified Savonius rotor	Bach	Fig. 5-6	2	1	2	120000	150000	0,77	0	124	0	0,196	0,180	0,976	0,970	Linear
	Bach	Fig. 5-6	2	1	2	120000	150000	0,77	0	124	0,1	0,571	0,508	0,977	0,973	Linear
	Bach	Fig. 5-6	2	1	2	120000	150000	0,77	0	124	0,16	0,000	0,000	0,897	0,892	No correlation
	Bach	Fig. 7-8	2	1	2	120000	150000	0,6	0	124	0	0,000	0,000	0,988	0,981	No correlation
	Bach	Fig. 7-8	2	1	2	120000	150000	0,6	0	124	0	0,040	0,061	0,995	0,994	Linear
	Bach	Fig. 7-8	2	1	2	120000	150000	0,6	0	124	0	0,151	0,104	0,981	0,975	Linear
	Bach	Fig. 7-8	2	1	2	120000	150000	0,6	0	124	0	0,342	0,418	0,994	0,985	Linear
	Bach	Fig. 9-10	2	1	2	120000	150000	0,7	0	110	0	0,168	0,156	0,945	0,942	Linear
	Bach	Fig. 9-10	2	1	2	120000	150000	0,7	0	124	0	0,060	0,080	0,995	0,994	Linear
	Bach	Fig. 9-10	2	1	2	120000	150000	0,7	0	135	0	0,693	0,744	0,984	0,978	Linear
	Bach	Fig. 9-10	2	1	2	120000	150000	0,7	0	150	0	0,326	0,332	0,954	0,931	Linear
	Bach	Fig. 11-12	2	1	2	120000	150000	0,7	0	124	0	0,077	0,091	0,995	0,994	Linear
	Bach	Fig. 11-12	2	1	2	120000	150000	0,7	0	124	0	0,585	0,631	0,994	0,993	Linear
	Bach	Fig. 11-12	2	1	2	120000	150000	0,7	0	124	0	0,056	0,065	0,996	0,996	Linear
	Bach	Fig. 14	2	1	4	80000	150000	0,2	0	124	0	0,308	0,329	0,983	0,980	Linear
	Conventional	Fig. 16	2	1	3	100000	150000	1	0	180	0,15	0,295	0,302	0,984	0,979	Linear
	Bach	Fig. 16	2	1	3	100000	150000	1	0	135	0	0,319	0,319	0,988	0,988	Linear
	Bach	Fig. 16	2	1	3	100000	150000	1	0	135	0	0,424	0,426	0,981	0,981	Linear
	Bach	Fig. 19	2	1	4	77600	150000	0,77	0	124	0	0,280	0,280	0,986	0,986	Linear
Kamoji et al. 2009b Helical SWT	Helical	Fig. 5,6	2	1	2	120000	150000	1	90	180	0	0,663	0,799	0,944	0,919	Linear
	Helical	Fig. 5,6	2	1	2	120000	150000	0,88	90	180	0	0,400	0,402	0,996	0,993	Linear
	Helical	Fig. 5,6	2	1	2	120000	150000	0,96	90	180	0,1	0,560	0,617	0,994	0,981	Linear
	Helical	Fig. 5,6	2	1	2	120000	150000	1	90	180	0,16	0,473	0,474	0,991	0,966	Linear
	Helical	Fig. 8	2	1	6	57702	201958	0,88	90	180	0	0,429	0,446	0,985	0,981	Linear
	Helical	Fig. 9,10	2	1	2	120000	150000	0,88	90	180	0	0,350	0,349	0,997	0,993	Linear
	Helical	Fig. 9,10	2	1	2	120000	150000	0,96	90	180	0,1	0,516	0,564	0,995	0,982	Linear
	Conventional	Fig. 9,10	2	1	2	120000	150000	1	0	180	0,15	0,000	0,000	0,994	0,991	No correlation
Mercado-Colmenero et al. 2018 Helical SWT	Conventional	Fig. 11	2	1	14	66000	136000	1,618	0	180	0,326	0,835	0,766	0,875	0,869	Unclear
	Helical	Fig. 12	2	1	15	66000	142000	1,618	22,5	180	0,326	0,776	0,590	0,930	0,927	Unclear
	Helical	Fig. 13	2	1	14	66000	136000	1,618	45	180	0,326	1,192	0,627	0,963	0,932	Polynomial
	Helical	Fig. 14	2	1	9	34400	77500	1,618	0	180	0,343	0,576	0,576	0,576	0,576	Unclear